

## Complex aromatic hydrocarbons in Stardust samples collected from comet 81P/Wild 2

Simon J. CLEMETT<sup>1\*</sup>, Scott A. SANDFORD<sup>2</sup>, Keiko NAKAMURA-MESSENGER<sup>3</sup>,  
Friedrich HÖRZ<sup>4</sup>, and David S. MCKAY<sup>4</sup>

<sup>1</sup>ERC, Inc., Houston, Texas 77058, USA

<sup>2</sup>Astrophysics Branch, NASA Ames Research Center, Moffett Field, California 94305, USA

<sup>3</sup>Jacobs, Houston, Texas 77058, USA

<sup>4</sup>NASA Johnson Space Center, Houston, Texas 77058, USA

\*Corresponding author. E-mail: simon.j.clemett@jsc.nasa.gov

(Received 27 November 2007; revision accepted 25 June 2009)

---

**Abstract**—The successful return of the Stardust spacecraft provides a unique opportunity to investigate the nature and distribution of organic matter in cometary dust particles collected from comet 81P/Wild 2. Analysis of individual cometary impact tracks in silica aerogel using the technique of two-step laser mass spectrometry demonstrates the presence of complex aromatic organic matter. While concerns remain as to the organic purity of the aerogel collection medium and the thermal effects associated with hypervelocity capture, the majority of the observed organic species appear indigenous to the impacting particles and are hence of cometary origin. While the aromatic fraction of the total organic matter present is believed to be small, it is notable in that it appears to be N rich. Spectral analysis in combination with instrumental detection sensitivities suggest that N is incorporated predominantly in the form of aromatic nitriles (R–C≡N). While organic species in the Stardust samples do share some similarities with those present in the matrices of carbonaceous chondrites, the closest match is found with stratospherically collected interplanetary dust particles. These findings are consistent with the notion that a fraction of interplanetary dust is of cometary origin. The presence of complex organic N containing species in comets has astrobiological implications as comets are likely to have contributed to the prebiotic chemical inventory of both the Earth and Mars.

---

### INTRODUCTION AND BACKGROUND

From an organic astromaterials perspective, the importance of the Stardust mission and the samples that it returned derive from the role that cometary materials serve as a bridge between solar system materials and the interstellar medium (ISM). Our understanding of the origin and evolution of organic matter in both interplanetary and interstellar space is necessarily limited by the availability of samples for laboratory analysis and/or the environments and conditions under which diagnostic spectra can be obtained by remote sensing. Laboratory studies of carbonaceous and ordinary chondrites have, and continue to, provided a

wealth of data on the organic composition of primitive solar system materials and their evolution and synthesis through aqueous, thermal, and shock alteration (Gilmour 2005; Sephton 2005; Pizzarello et al. 2006). However, the picture they provide is necessarily incomplete as the dynamical evolution of meteorites into Earth-crossing orbits results in sample selection biasing (e.g., Scholl and Froeschle 1977). While there is persuasive evidence that a small fraction of the organics observed in the least altered carbonaceous chondrites do retain an isotopic signature of their interstellar precursors (e.g., Busemann et al. 2006; Nakamura-Messenger et al. 2006), conditions in the early solar nebula, at least in the chondrite forming region, are

expected to have lead to the destruction and/or reprocessing of a significant fraction of pre-existing interstellar organic matter (Sephton and Gilmour 2000; Sephton et al. 2004).<sup>1</sup> Our knowledge of interstellar organics is therefore based, to a large extent, on remote spectroscopic observations in conjunction with laboratory analysis of radiation processed interstellar ice analogs. Infrared absorption by, and emission spectra from, interstellar materials suggests that at least several components of the dust are carbonaceous (Allamandola et al. 1985; Sandford et al. 1992; Duley and Grishko 2003). Over 100 small molecular species, many of them C containing, have now been identified in interstellar and circumstellar gas clouds through their rotational and rovibrational spectra (Henning and Salama 1998). Finally, although no specific molecular assignment is possible, a vast and diverse population of polycyclic aromatic hydrocarbons (PAHs) are inferred to be responsible for the ubiquitous “unidentified” infrared emission bands near 3.28, 6.2, 7.6–7.9, and 11.2  $\mu\text{m}$  (attributed to C–H stretching, C–C stretching, and C–H bending modes, respectively) observed from many astronomical sources. It has been estimated that such PAHs could account for approximately 10% of the total estimated interstellar C budget making them the most abundant molecular species in the universe after  $\text{H}_2$  and CO (Salama et al. 1999). These PAHs are believed to form in the outflows of evolved stars (Cherchneff et al. 1992; Cherchneff 1995; Woods and Willacy 2007), and their role in producing these infrared emission bands has now become widely accepted (Leger and Puget 1984; Allamandola et al. 1985, 1999).

Due both to their small size and site of accretion in the outer reaches of the solar system, comets are believed to have escaped much of the aqueous, thermal, and shock alteration effects characteristic of the meteorite parent bodies. However, this does not imply that they are simply pristine agglomerations of interstellar matter. Remote spectroscopic observations of many comets near perihelion indicate that, while their abundance of volatile species does broadly parallel that of interstellar dust clouds they are not identical. Nevertheless large H ( $^1\text{H}/^2\text{H}$ ) and N ( $^{14}\text{N}/^{15}\text{N}$ ) isotopic anomalies observed in some stratospherically collected interplanetary dust particles (IDPs), some of which are inferred to be of cometary origin, have long suggested that comets are likely to have retained at least a partial

record of their original presolar volatile inventory. This is supported by the detection of similar isotopic anomalies in samples returned from comet 81P/Wild 2 by the Stardust mission (McKeegan et al. 2006). Consequently laboratory analysis of cometary organic matter can offer a unique perspective on the nature and evolution of the interstellar compounds during the formation of our solar system as well as providing a missing link to the progenitor dense molecular cloud from which the nascent solar system formed.

### Cometary Organic Matter

Until the return of samples from comet 81P/Wild 2, our understanding of the organic inventory of comets was based on three broad groups of measurements (for a comprehensive review see Altwegg et al. 1999):

- Spectroscopic observations of comets and their comae close to perihelion.
- Laboratory analysis of irradiated interstellar ice analogs under relevant astrophysical conditions.
- In situ mass spectrometer measurements of cometary grains made by the Vega I/II and Giotto spacecraft during their 1986 flyby of comet 1P/Halley.

As a comet approaches perihelion, sublimation of surface ice releases dust grains and gas phase species into the local environment of the comet to form the coma. Subsequent irradiation by the solar ultraviolet (UV) radiation field leads to the rapid photodissociation and ultimately ionization of many of the gas phase species present in the coma. These ions can then undergo further modification by reaction with neutral species in complex sequences of ion-molecule reactions, before their interaction with the solar wind sweeps away from the comet to form an ion tail. This complicated chain of reactions makes it difficult to reconstruct the nature and abundance of the unobserved parent molecules in the nucleus from the spectroscopic observations of daughter molecular species visible in both the coma and the ion tail. Hence, the precise nature of the organic component in comets cannot be revealed from such measurements alone, although a range of simple organics species have been identified including  $\text{CH}_4$ ,  $\text{C}_2\text{H}_2$ ,  $\text{C}_2\text{H}_6$ ,  $\text{HCHO}$ ,  $\text{CH}_3\text{OH}$ ,  $\text{CH}_3\text{CN}$ ,  $\text{NH}_2\text{CHO}$ ,  $\text{HCOOH}$ ,  $\text{HC}_3\text{N}$ ,  $\text{HCOOCH}_3$  (e.g., Bockelée-Morvan et al. 2000). Identification of more complex species is more speculative, an emission band near 3.28  $\mu\text{m}$  has been observed in some comets (Davies et al. 1991; Bockelée-Morvan et al. 1995) and tentatively attributed to gas phase PAHs, although emissions from other species particularly  $\text{CH}_4$  and  $\text{OH}^\bullet$  may also contribute at this wavelength. No PAH bands were observed in comet Hale-Bopp, either from the ground

<sup>1</sup>It is noted, however, that alternative interpretations have been advocated although not yet widely accepted; suggesting chondrites are composed of essentially two components—a processed, organic free, high temperature material, and a primitive, relatively unprocessed component that dominates the matrix (e.g., Alexander et al. 2007. The origin and evolution of chondrites recorded in the elemental and isotopic compositions of their macromolecular organic matter).

or with the European Space Agency (ESA) Infrared Space Observatory (ISO), but the ISO spectra were obtained, however, at relatively large heliocentric distances ( $>2.7$  AU) where PAHs would not have been emitting efficiently. On the other hand, emission spectra of comet 1P/Halley in the 275–710 nm range observed by the Vega II spacecraft did show the presence of a broadband emissive feature between 340 and 390 nm with three peaks at 371, 376, and 382 nm. As the intensity of these features correlated with decreasing distance to the comet nucleus, these spectral features are presumed to be derived from a parent molecular species. One candidate species for the source of this feature is phenanthrene ( $C_{14}H_{10}$ ), with pyrene ( $C_{16}H_{10}$ ) as a possible secondary minor component (Clairemidi et al. 2004). Unambiguous confirmation requires a more rigorous understanding of how PAHs are released from cometary refractories into the gas phase, the excitation mechanism that subsequently leads to infrared (IR) emission (thought to be dominated by electronic pumping in the UV followed by intermode conversion to excitation vibrational modes), and the lifetime of gas phase PAHs in cometary comae (Joblin et al. 1997).

Dust-impact time-of-flight mass spectrometers were flown onboard the Vega I/II (PUMA instrument, von Hoerner & Sulger GmbH, Schwetzingen, Germany) and Giotto (PIA instrument, Max-Planck-Institut-fuer-Kernphysik, Heidelberg, Germany) spacecraft during their 1986 flybys of comet 1P/Halley. In all, 5000 individual particle mass spectra were acquired at distances to the comet nucleus ranging from 8000 to 180,000 km. When taken as a whole, some of the physical properties of Halley dust particles can be inferred. Kissel and Krueger (1987) proposed a model in which a typical dust particle is composed of a somewhat porous chondritic mineral core ( $\rho$  about  $1\text{--}2\text{ g cm}^{-3}$ ) that is embedded within a mantle of refractory organic matter ( $\rho$  about  $0.3\text{--}1\text{ g cm}^{-3}$ ). Both the chondritic mineral core and refractory organic matter represent the two endmembers for a distribution of particles based on the relative proportions of each endmember. Approximately 30% of the dust particles had spectra showing only the light elements, C, H, O, N (the so called “CHON” particles), while approximately 35% showed element distributions consistent with only a chondritic mineral phase. The remaining approximately 35% showed both. The mass range of detected particles from the Vega I PUMA and Giotto PIA instruments was estimated to range from  $3 \times 10^{-16}$  to  $3 \times 10^{-10}$  g [this has been more recently adjusted to  $5 \times 10^{-17}$  to  $3 \times 10^{-12}$  g (Fomenkova 1999)]. Photofragmentation of cometary CHON particles has been proposed to account for the extended sources seen for many molecules and radicals in the coma, in

particular CO,  $C_2$ ,  $H_2CO$ , CN, and  $NH_2$ . Specifically, to account for the coma sources of CO and  $H_2CO$ , and other regular peaks in the mass spectra of “CHON” particles seen by Giotto, it has been proposed that a substantial fraction of the CHON material consists of the formaldehyde polymer, polyoxymethylene (POM,  $[-CH_2-O-]_n$ ) (Huebner et al. 1987). Other potential candidates include hexamethylenetetramine (HMT,  $C_6H_{12}N_4$ ) (Bernstein et al. 1995), polyaminocyanomethylene (PACM,  $[-(NH_2)C(CN)-]_n$ ) (Rettig et al. 1992), and PAHs (Moreels et al. 1994). However, as Charnley et al. (2002) noted, “. . . *this material cannot be unequivocally identified via spectroscopy of the coma, and we must wait until the Stardust mission returns a sample of comet dust to the Earth for laboratory analysis before we can properly understand the nature of the CHON grains.*”

## EXPERIMENTAL TECHNIQUE AND SAMPLE PREPARATION

### Two-Step Laser Mass Spectrometry

Many different analytical approaches have been used to characterize organic matter in astromaterials and consequently it can be difficult to establish quantitative comparisons between samples because of the often disparate spatial resolutions, selectivity, and sensitivities of the different analytical techniques. We focus primarily on those results that have been obtained with the  $\mu$ ltra- $L^2$ MS instrument located at NASA Johnson Space Center. The technique of two-step laser desorption/laser ionization mass spectrometry ( $L^2$ MS) has provided a versatile method for the detection of aromatic/conjugated organic molecules in microscale and/or heterogeneous samples. It provides in situ characterization of a sample at the tens of microns resolution with sub-femtomole ( $<10^{-18}$  mole) detection limits. Unlike allied surface analysis techniques such as secondary ion mass spectrometry (SIMS),  $L^2$ MS is far less susceptible to the extensive fragmentation and/or surface matrix effects associated with combining both the desorption and ionization steps into one.

The underlying concept of  $\mu$ ltra- $L^2$ MS, namely that of two-step laser mass spectrometry, is briefly summarized here (for a more detailed description see Clemett and Zare 1996). In step one, a spatially focused IR laser pulse (typically  $\lambda = 10.6\text{ }\mu\text{m}$ ) is used to desorb material nonthermally from the sample substrate that is placed within a high vacuum chamber. The laser desorption fluence is carefully controlled (typically  $<10^6\text{ W cm}^{-2}$  with  $dT/dt$  about  $10^8\text{--}10^{11}\text{ K s}^{-1}$ ) to avoid plasma breakdown. In other words, desorbed material is liberated from the sample substrate exclusively as neutral

species. After an appropriate time delay that allows desorbed species to expand away from the substrate surface, a second UV laser pulse orthogonal to the IR laser pulse and parallel to the sample surface is directed through the desorbed neutrals, photoionizing specific molecules within the desorbed plume. By allowing laser photoionization to occur within the source region of a modified Wiley-McLaren ion extractor, ionized species generated by the photoionization process are separated from the neutral desorption plume and injected into a reflectron time-of-flight mass spectrometer. Under appropriate laser wavelength (typically  $\lambda = 266$ ) and fluence (approximately  $10^9$ – $10^{15}$  W cm<sup>-2</sup>) and pulse duration (approximately  $10^{-9}$ – $10^{-12}$  s), the UV laser pulse can achieve efficient “soft” ionization of selected classes of organic species. That is, ionization occurs with minimal fragmentation, where energy in excess of that necessary for ionization is transferred to the kinetic energy of the liberated photoelectron. The L<sup>2</sup>MS technique has already been used to establish the presence of aromatic hydrocarbons in a wide variety of astromaterials including: [1] meteoritic acid residues (Kovalenko et al. 1992); [2] carbonaceous and ordinary chondrites (Hahn et al. 1988; Zenobi et al. 1989, 1992); [3] Martian meteorites (McKay et al. 1996; Clemett et al. 1998b); [4] Antarctic micrometeorites (Clemett et al. 1998a); [5] interplanetary dust particles (Clemett et al. 1993); [6] interstellar graphite grains (Messenger et al. 1998); and [7] laboratory synthesized interstellar ice residues (Bernstein et al. 1999; Elsila et al. 2005).

### Stardust and Reference Samples

During the preliminary examination period, the L<sup>2</sup>MS technique was applied to the analysis of a broad range of Stardust samples and associated blanks that, for the purposes of discussion, can be divided into three groups:

1. Contamination controls;
2. Al foil microcraters;
3. Aerogel tracks.

Contamination controls included not only aerogel and Al foil flown onboard the sample return capsule but which were not directly exposed to the 81P/Wild 2 particle flux, but also postflight samples of the sample return capsule including the pyrolytic C ablator heat shield and atmospheric vent filter. Complete inventories of samples analyzed to date are presented in Table 1. As little to no organic matter was observed in Al foil microcraters above levels that can reasonably be accounted for by terrestrial contamination issues, this manuscript is focused specifically on the analysis of cometary particle impact features in aerogel. The results

Table 1. Stardust samples analyzed by two-step laser mass spectrometry.

Group I: Flight blanks	
WCARMIICPN,0,10	Flight aerogel flown but not exposed to comet
WCARMIICPN,0,11	. . .0,6 & . . .0,10 top surface
WCARMIICPN,0,6	. . .0,7 & . . .0,11 bottom surface
WCARMIICPN,0,7	
CO126N,4	Al foil
CO2102N,2	Al foil
C2092E,4	Al foil
Flight spares	One sample from each batch of aerogel that was ultimately installed on the WISCER grid
Group II: Al foil	
CO2102N,1	Al Foil with impact crater
C2107,W,1,4	Al Foil with impact crater
Group III: Aerogel	
FC12-2-16 Fragment 12A-3	Cross sectioned keystone aerogel track
C2115, Track 22	Cross sectioned keystone aerogel track
CF12,0,16,1,0	Terminal particle sectioned and in epoxy butt
CF12,0,16,1,7	Terminal particle, 3 TEM sections on Si
C044	Cross sectioned impact track
C2115,26,22 track 6	Cross sectioned impact track bulb section
C2115,28,21 track 5	Cross sectioned impact track
C2115,19,45,0,0	Cross sectioned impact track bulb section
C2054,9,35,0,0	Aerogel fragment with particles on surface

of blank analyses and contamination controls will be addressed in detail in a separate future manuscript.

Aerogel samples containing cometary impact features that were allocated for L<sup>2</sup>MS analysis were provided either as “box-cuts” from a given tile (e.g., C2115 Track 22) or as loose aerogel fragments recovered during the opening of the sample return capsules (e.g., FC-12-2-16 Fragment 12A-3). In either case, the physical dimensions of the aerogel sample were typically on the order of several hundred to a thousand microns along any given dimension.

One of the primary virtues of the L<sup>2</sup>MS technique is that it requires only minimal sample preparation, and analysis is only minimally destructive such that the same sample is subsequently suitable for analysis by other microanalytical techniques. In the case of ultra-L<sup>2</sup>MS the only prerequisite for analysis is that the sample be securely attached to a 1 inch diameter stainless steel sample platter. Meeting this requirement

for both foils and TEM thin-sections on Si is trivial and mounting can be conveniently achieved using the low melting point mount thermopolymer (Crystalbond™ 555, SPI Supplies Division, Structure Probe, Inc., West Chester, PA, USA). Unfortunately this approach is unsuitable for aerogels because the capillary action of aerogel causes wicking of the mount adhesive into the aerogel bulk that subsequently begins to collapse due to surface tension forces exerted by the mount adhesive. The net effect is loss of structural integrity and irreversible contamination of the aerogel. As a consequence, for the  $\mu$ tra-L<sup>2</sup>MS measurements, we developed a passive “organics free” friction mounting technique whereby the aerogel is sandwiched between a Au 200 Mesh TEM grid (on the bottom) and an etched stainless steel mesh (50  $\mu$ m bars spaced at 500  $\mu$ m intervals) as detailed in Fig. 1. For instrument calibration purposes, every Stardust sample analyzed was co-mounted with either one or two references that consisted of pulverized carbonaceous chondrite matrix from either Orgueil (CI1), Tagish Lake (CI2), Murchison (CM2), or Allende (CV3), that we pressed in to Au foil. The reference samples provided a known and well characterized mass spectrum that could be used to calibrate the time-of-flight mass spectrometer prior to each aerogel analysis, as well as provide a suitable context in which to compare aerogel spectra.

## RESULTS

Before proceeding to the analysis of individual ultra-L<sup>2</sup>MS spectra, it is prudent to make a couple of qualifications regarding peak intensities. In general for ultra-L<sup>2</sup>MS mass spectra, peak intensities are reported in arbitrary units. This is performed in order to emphasize that while the relative distribution of mass peaks obtained from a sample is invariant (within limits) to both the nature of the sample and instrument variables, this is not true of absolute intensities. For example, two samples of the same material but with different surface areas will give identical spectra distributions but will have different overall intensities. Only when identical sample preparation and instrument conditions are used for analysis, is it valid to compare absolute intensities between different spectra.

### Carbonaceous Chondrite Reference Samples

Well averaged spectra of the Orgueil (CI1), Tagish Lake (CI2), Murchison (CM2), and Allende (CV3) carbonaceous chondrite reference samples are shown in Fig. 2. These spectra were obtained both contemporaneously with, and under exactly the same experimental conditions as, those used for the analysis

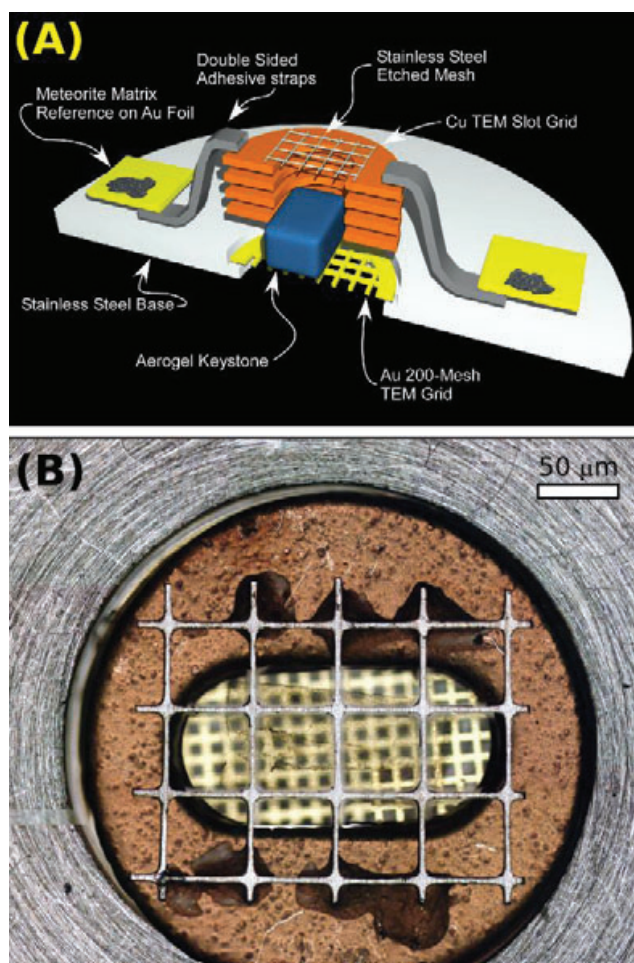


Fig. 1. A) Mounting scheme used for the analysis of aerogel tracks in the  $\mu$ tra-L<sup>2</sup>MS instrument. The aerogel keystone is sandwiched between a Au 200 Mesh TEM grid and an etched stainless steel mesh. The spacing between the lower Au grid and the top mesh is determined by the stacked copper TEM slot grids. The slot grids and stainless mesh are bonded together using Crystalbond™ 555 thermoadhesive prior to placement on the sample. The number of slot grids is chosen such that when mounted, the aerogel is under slight compression to prevent lateral movement of the sample during instrument loading and analysis. The mounting procedure involves transfer of the aerogel keystone onto the Au grid using a glass needle. Once the sample is correctly oriented, the upper slotted grid and stain steel mesh assembly is lowered down and over the sample. The edges of the uppermost slot grid are then anchored into position on the stainless steel base holder using two thin slivers of SEM carbon adhesive tape. After the aerogel is mounted, reference samples of carbonaceous chondrite matrix pressed onto Au foil are attached to either side of the aerogel on top of the SEM adhesive tape. B) Optical image of Stardust aerogel Sample C2115 Track 22 mounted and ready for analysis by the JSC ultra-L<sup>2</sup>MS instrument.

of Stardust related samples. They represent, with the possible exception of stratospherically collected interplanetary dust particles (IDPs), some of the least

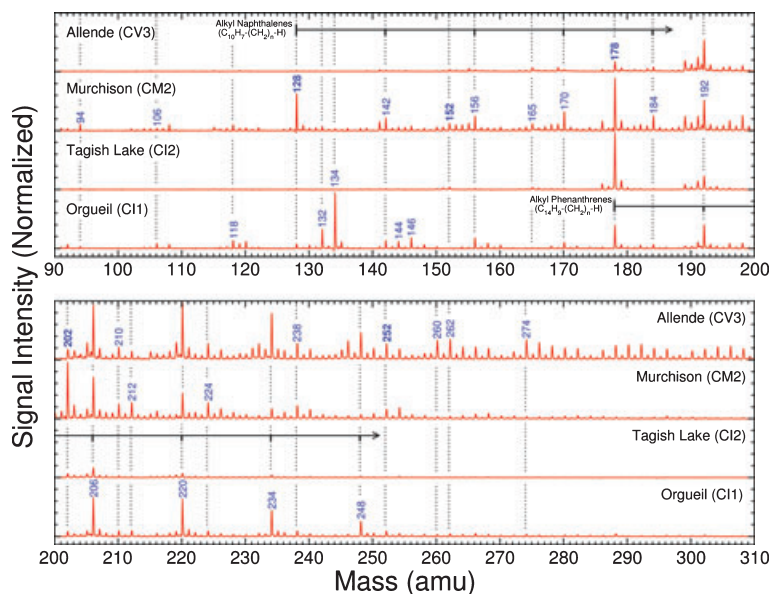


Fig. 2. Reference spectra over the mass range 90–310 amu for matrix samples of the CI, CM, and CV chondrite classes. All spectra were acquired at the same time and under identical experimental conditions to those in the analysis of the Stardust samples. Each spectrum has been normalized to its strongest peak for comparison purposes. With the exception of stratospherically collected interplanetary dust particles (IDPs), chondrites such as Tagish Lake (CI2) and Murchison (CM2) are the least altered, and hence most primitive, solar system materials available for laboratory analysis. Orgueil (CI1) has undergone a greater degree of parent body aqueous alteration in comparison with either Tagish Lake or Murchison, while Allende (CV3) has undergone a greater degree of parent body thermal alteration.

altered and hence most primitive solar system materials available for laboratory analysis.

In general the chondrite spectra are characterized by multiple overlapping alkylation series of simple 1–5 ring PAH parent species. Successive addition of alkyl groups,  $-(\text{CH}_2)-$ , gives rise to series of mass peaks regularly spaced at 14 amu, extending to higher mass from the parent PAH and can be represented by the chemical formula  $\text{Ar}-(\text{CH}_2)_n-\text{H}$  where  $n = 0$  corresponds to the parent aromatic species,  $\text{Ar}-\text{H}$ , and  $n = 1, 2, 3, \dots$  are the alkylated homologs. For carbonaceous chondrites, two alkylation series tend to be particularly prevalent—the 2-ring and 3-ring PAHs naphthalene (128 amu;  $\text{C}_{10}\text{H}_8$ ) and phenanthrene (178 amu;  $\text{C}_{14}\text{H}_{10}$ ), respectively. These alkylation series are shown in Fig. 2 and account for peaks at 128 ( $n = 0$ ), 142, 156, 170, 184, ..., and 178 ( $n = 0$ ), 192, 206, 220, 234 amu. As a general rule of thumb in the  $\text{L}^2\text{MS}$  analysis of chondritic meteorites, the higher the petrographic number of the chondrite analyzed the more the PAH mass envelope is shifted to higher masses (Clemett 1996). For example, Allende (CV3) in comparison with Orgueil (CI1) has virtually no low molecular weight 1–3 ring PAHs such as benzene ( $\text{C}_6\text{H}_6$ ; 78 amu), naphthalene ( $\text{C}_8\text{H}_{10}$ ; 128 amu), acenaphthylene ( $\text{C}_{12}\text{H}_8$ ; 152 amu), and fluorene ( $\text{C}_{13}\text{H}_{10}$ ; 166 amu). The underlying causes of this pattern are the differences in

both aqueous and thermal alteration (and possibly shock?) experienced during parent body alteration. In the case of thermal processing, both evaporative loss due to the greater thermal volatility of lower molecular weight PAHs, and thermally induced free radical polymerization (i.e.,  $2\cdot\text{Ar}-\text{H} \rightarrow 2\cdot\text{Ar}' + 2\cdot\text{H}' \rightarrow \text{Ar}-\text{Ar} + \text{H}_2$ ) would both have contributed to the high mass shift of PAH mass envelope. Hence, the variation in the mass distribution of PAHs in chondritic meteorites can be correlated to the evolution of the parent body from which the meteorite originated.

### Stardust Aerogel Tracks

For C2115 Track 22 (Fig. 3) multiple averaged spectra were all acquired starting close to the track entrance point into the aerogel, and extending several hundred microns into the aerogel. Within experimental uncertainties, the mass distribution of organic species within the track did not appear to show any compositional variation with the depth of penetration; however, we would add the caveat that there is a pronounced reduction in the total signal observed with increasing penetration depth into the aerogel. At a penetration depth of approximately 1000  $\mu\text{m}$ , the total organic signal is reduced by an order of magnitude relative to that observed near the entrance point. The

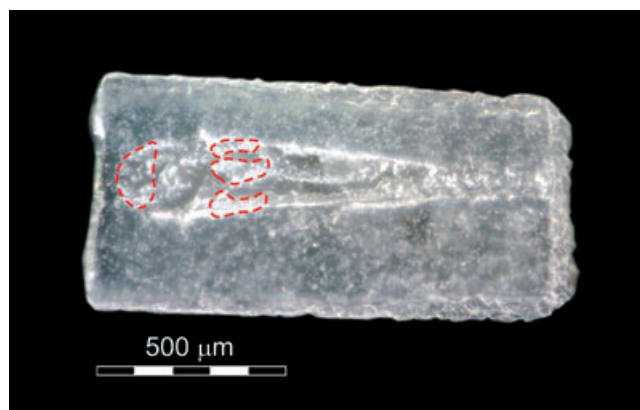


Fig. 3. Stardust aerogel sample C2115 Track 22 prior to sample mounting. The rectangular aerogel block in which the track bulb is embedded is about 1300  $\mu\text{m}$  in length, about 550  $\mu\text{m}$  in width, and about 200  $\mu\text{m}$  in thickness. The left hand edge of the aerogel block corresponds to upper exposed surface of the aerogel cell from which the sample was removed, and the impacting cometary particle entered from left to right, in the plane of the image to create the observed impact bulb. The sample was cut such that the track bulb was split evenly in half along its major axis such that the upper surface of this sample has the exposed surface of the track bulb. Four regions within the interior of the excavated track have been outlined; these correspond to the regions of the track analyzed by  $\mu\text{L}^2\text{MS}$  that were summed to produce the mass spectrum shown in Fig. 5. Subsequent regions (not shown) were also analyzed to assess background levels of organics in the surrounding aerogel and at greater depth down the track.

physical sides of the track also do not serve as the demarcation point for organic matter associated with the track; rather there is a monotonic decrease in the total organic signal moving out perpendicularly from the track axis. This apparent injection of organic matter associated with the track forming event typically extends to at least several track diameters. This extended distribution of the organics was previously noted from whole track maps of the intensity of infrared absorption in aliphatic C–H stretching mode bands (Sandford et al. 2006). Given the volatility of some organic species observed in this extended halo, it is difficult to say whether this diffusion occurred in a single short pulse during the creation of the impact event or whether it is representative of an ongoing slow diffusion. In the latter case, we can expect some temporal variation with length of curation in the nature of any organic matter observed in Stardust aerogels. This is a possibility that should be monitored by future measurements.

For aerogel sample FC-12-2-16 Fragment 12A-3 (Fig. 4), the orientation of the track bulb is well defined with respect to the impact vector, but the fraction of the track volume represented by the section is not well

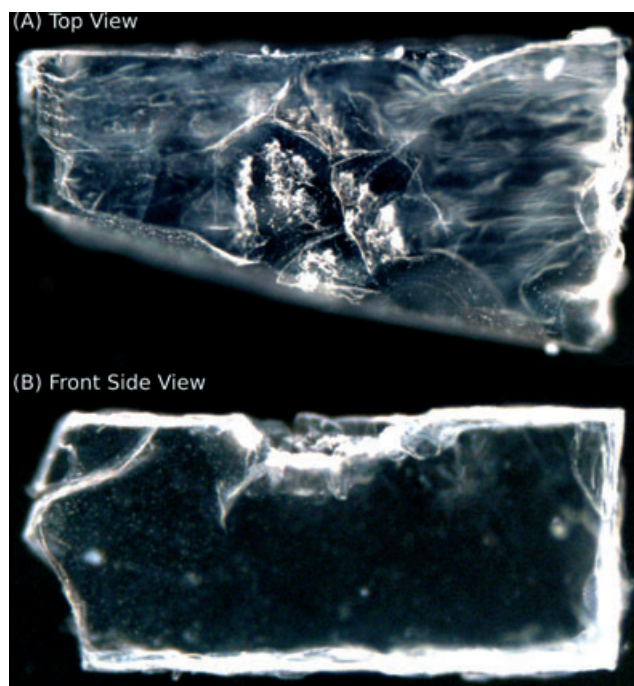


Fig. 4. Top and side views of Stardust aerogel sample Track FC12-2-16 Fragment 12A-3 taken prior to sample mounting. The trapezoidal aerogel block is approximately 1750  $\mu\text{m}$  in length with a width at one end of approximately 1000  $\mu\text{m}$  decreasing to approximately 500  $\mu\text{m}$  at the opposing end, and a thickness of approximately 800  $\mu\text{m}$ . The lower center of the upper surface transects a bulb shaped impact feature approximately 800  $\mu\text{m}$  in diameter. The exposed surface of the bulb is peppered with numerous micron sized particulates that appeared optically dark in reflection. The direction vector of the impact particle is not well constrained as this sample came from a loose fragment of aerogel recovered from the sample return capsule.

defined. Multiple spectra were acquired from multiple regions in the center of the track bulb. Given the extremely high surface area of silica aerogel combined with its propensity to adsorb volatile organic species, this sample was maintained under vacuum ( $<10^{-7}$  torr) within the  $\mu\text{L}^2\text{MS}$  instrument for a period of several weeks. During this time, spectra were periodically acquired in order to assess any temporal variations that would be indicative of the possibility of sample contamination by a virtual leak in the analysis chamber. No evidence of contamination was found.

Well averaged organic mass spectra obtained from Stardust aerogel impact tracks C2115 Track 22 and FC-12-2-16 Fragment 12A-3 are shown separately in Figs. 5 and 6. As the spectra are broadly similar, we will not discuss each spectrum separately, but rather discuss them collectively and, where necessary, point out any differences. Both aerogel tracks demonstrate a rich spectral complexity, indicating the presence of a complex assemblage of organic species. The primary

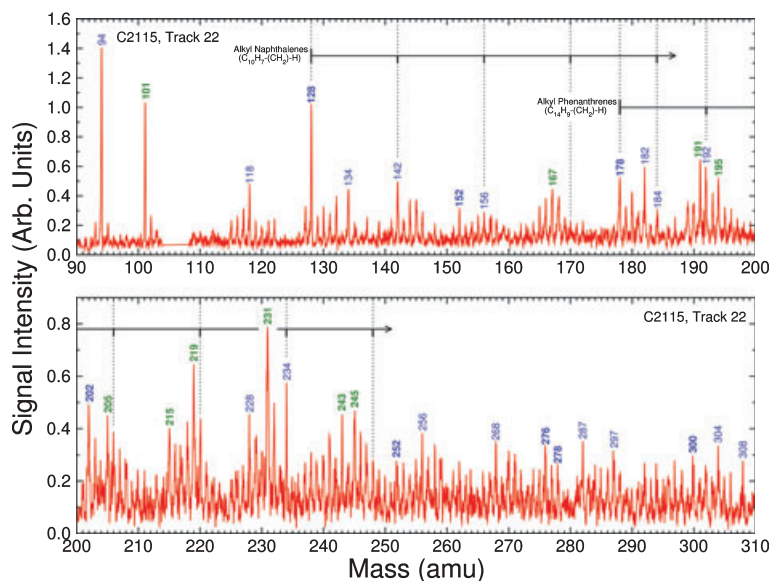


Fig. 5.  $\mu$ ltra- $L^2$ MS spectrum of Stardust aerogel sample C2115 Track 22 over the mass range 90–310 amu. The spectrum represents the summed signal from the four regions of the upper track surface as indicated in Fig. 3. Peaks in the mass window 104–108 amu have been removed as 1,3-dimethyl benzene ( $\text{CH}_3\text{-C}_6\text{H}_4\text{-CH}_3$ ; 106 amu) was used as a mass calibration and photofragmentation check prior to sample analysis. Prominent peaks are mass indexed and the labels are color coded. Peaks labeled in **bold blue** correspond to simple parent polycyclic aromatic hydrocarbons (PAHs) (e.g., naphthalene; 128 amu) while those in normal blue correspond their alkylated homologs (e.g., 1-methyl naphthalene; 142 amu). Peaks labeled in **bold green** correspond to prominent odd mass N containing PAHs (N-PAHs), which are not observed in the spectra of carbonaceous chondrites (see Fig. 1). Note that, for a number possible of reasons, not all prominent peaks are necessarily labeled. In some cases, this represents uncertainty in assignment and that the peak is not part of a homologous series. In other cases, a peak may not be labeled as it represent a secondary fragment ion, e.g., an  $\text{-H}$  or  $\text{H}_2$  loss peaks formed during photoionization, or is simply a  $^{13}\text{C}$  molecular isotopomers of a marked peak. Two PAH alkylation series corresponding to  $\text{C}_n$ -alkyl naphthalene and  $\text{C}_n$ -alkyl phenanthrene are also indicated, both alkylation series are prominent in the spectra obtained from both ordinary and carbonaceous chondrites.

mass envelope for C2115, Track 22 (Fig. 5) spans a mass range of approximately 100–350 amu, while that for FC-12-2-16 Fragment 12A-3 (Fig. 6) ranges from approximately 150 to 350 amu and shows a weaker, secondary mass envelope between approximately 500 and 700 amu. Clearly neither spectrum shows a direct match to any of the reference carbonaceous chondrite spectra that were acquired under identical conditions (Fig. 2). Nevertheless, there are some underlying commonalities. For example, both aerogel tracks show well developed peak sequences characteristic of alkylated phenanthrenes (e.g., 178, 192, 206, 220, 234 amu), while C2115 Track 22 also exhibits a peak series for alkylated naphthalenes (e.g., 128, 142, 156, 170 amu). However, the most distinctive feature of both cometary spectra, a feature that is notably absent in carbonaceous chondrite spectra, is the abundance of odd mass peaks, specifically those at 155, 167, 181, 191, 195, 203, 205, 215, 217, 219, 221, 229, 231, 243, and 245 amu. At this point, it is important to reiterate that because of the relatively “soft” nature of the  $L^2$ MS photoionization process, the vast majority of peaks in an  $L^2$ MS spectrum arise from radical even mass

molecular parent ion peaks rather than odd mass daughter fragment ions. For example, the  $L^2$ MS spectrum of 1,4-dimethylbenzene ( $\text{CH}_3\text{-C}_6\text{H}_4\text{-CH}_3$ ) gives rise to a single dominant radical molecular ion peak ( $[\text{CH}_3\text{-C}_6\text{H}_4\text{-CH}_3]^+$ ) at 106 amu, with only a small contribution from the odd mass fragment ( $[\text{CH}_3\text{-C}_6\text{H}_4]^+$ ) at 91 amu. Under these conditions, the so-called “Nitrogen Rule” is applicable. This notes that for most organic molecules, there is a serendipitous odd–even correspondence between the masses of the most abundant isotope of the constituent elements and their valence. In other words, they are either both even- or odd-numbered (e.g.,  $^1\text{H}$ ,  $^{16}\text{O}$ , and  $^{12}\text{C}$ , have valencies of 1, 2, and 4, respectively). The notable exception is N with an odd valence (i.e., trivalent) but an even mass primary isotope (i.e.,  $^{14}\text{N}$ ). As a consequence, an organic compound containing one N atom (or any odd number) will have an odd mass parent molecular ion, while an organic compound containing two N atoms (or any even number) will have an even mass parent molecular ion. Hence, the odd mass peaks observed in both aerogel track spectra, if we permit the assumption that they are parent molecular ions, correspond to

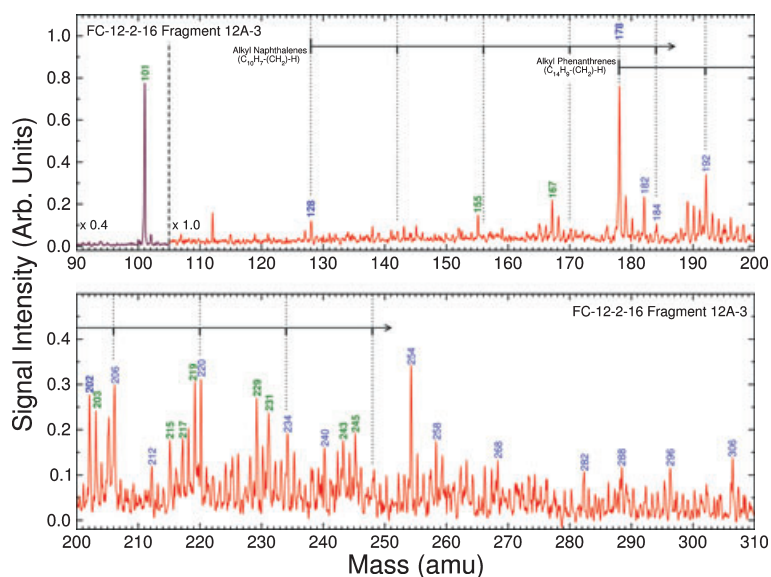


Fig. 6.  $\mu$ LA- $L^2$ MS spectrum of Stardust aerogel sample FC-12-2-16 Fragment 12A-3 over the mass range 90–310 amu. The spectrum represents the summation of all spectra obtained within the track bulb and signal intensities are plotted relative to that for sample C2115 Track 22 as shown in Fig. 5. Prominent peaks are mass indexed using the same color coding scheme as employed in Fig. 5; in addition, the naphthalene and phenanthrene alkylation peak series are also indicated. The mass window from 90–105 amu is scaled by a factor 0.4 relative to that from 105–310 amu due to the presence of a single strong peak at 101 amu that is native to the sample.

aromatic species with a single N containing functional group attached. As aromatic N-heterocycles tend to have low photoionization cross sections under the experimental conditions used (266 nm photoionization), the detection limits for these species are in general very poor compared with their homocyclic isomers. For example, the detection sensitivities for phenanthrene ( $C_{14}H_{10}$ ) and its analogous N-heterocycle 6-phenanthridine ( $C_{13}H_9N$ ) by  $L^2$ MS at 266 nm are approximately 1:2000 (Clemett 1996).<sup>2</sup> This makes it unlikely that the observed odd mass species represent N-heterocycles, i.e., species with N within the aromatic skeleton. It should be noted that this does not preclude their presence, but rather under the experimental conditions used for the  $L^2$ MS analyses, they would not have been detected. This leaves species of the form  $Ar-(CH_2)_n-[N]$  where [N] is a N containing functional group. If we exclude ionic species such as diazonium salts ( $-N^+\equiv N$ ), then possible forms for [N] are [1]

<sup>2</sup>This part is due to decrease in the energy gap between the highest occupied molecular orbital (HOMO) and lowest unoccupied molecular orbital (LUMO) on replacing an aromatic C with N. This results in a shift of in the maximum of the UV adsorption to longer wavelengths making harder to photoionize at the fixed wavelength of 266 nm used here. For the example of phenanthrene and phenanthridine, the HOMO-LUMO energy gaps are approximately 8.20 eV (Bleeker et al. 1998. Comparative ecotoxicity of NPAHs to larvae of the midge *Chironomus riparius*), and 8.37 eV (Mekenyan et al. 1994. QSARs for photoinduced toxicity: I. Acute lethality of polycyclic aromatic hydrocarbons to *Daphnia magna*), respectively.

nitrile/isonitrile ( $-C\equiv N/-N\equiv C$ ); [2] cyanate/isocyanate ( $-OCN/-NCO$ ); [3] amide ( $-CO_2NH_2$ ); [4] amine ( $-NH_2$ ); and [5] nitro ( $-NO_2$ ). If we restrict Ar to simple stable five and six ring aromatics, we can construct a table of possible parent ion masses that could be observed (Table 2). From this table, we can see that nearly all the observed odd mass peaks with the exception of peaks at 215, 229, and 243 amu could be accounted for by  $C_n$ -aromatic nitriles/isonitriles. The 14 amu spacing between many of the peaks is consistent with methylene insertion ( $-CH_2-$ ; 14 amu) suggesting several overlapping alkylation series, which also supports the idea of a single common N functionality. Indeed, if we allow unsaturation of alkyl groups, then the peaks at 229 and 243 amu would be also consistent with nitriles/isonitriles of the form phenanthrene- $(CH=CH)-CN$  and phenanthrene- $CH_2-(CH=CH)-CN$ .

### Stardust Aerogel Witness Control

During the nearly seven-year flight and return phase of the Stardust spacecraft, several contamination routes had the potential to influence the organic record of the comet encounter preserved by the aerogel collection medium. In no particular order, these are (1) volatile organics degassed from spacecraft components as a consequence of vacuum exposure and solar UV irradiation; (2) hydrazine and residual organics from

Table 2. Possible mass assignments for Ar-(CH<sub>2</sub>)<sub>n</sub>-[N] species (mass in bold observed in Stardust samples).

PAH parent	Mass (amu)	-CN/-NC	-OCN/-NCO	-CONH <sub>2</sub> <sup>a</sup>	-NH <sub>2</sub> <sup>b</sup>	-NO <sub>2</sub>
Benzene	78	103	119	121	93	123
C <sub>1</sub> -Benzene	92	117	133	135	107	137
C <sub>2</sub> -Benzene	106	131	147	149	121	151
Indene	116	141	157	159	131	161
C <sub>3</sub> -Benzene	120	145	161	163	135	165
Naphthalene	128	153	169	171	143	173
C <sub>1</sub> -Indene	130	<b>155</b>	171	173	145	175
C <sub>1</sub> -Naphthalene	142	<b>167</b>	183	185	157	187
C <sub>2</sub> -Indene	144	169	185	187	159	189
Acenaphthylene	152	177	193	<b>195</b>	167	197
Biphenyl	154	179	<b>195</b>	197	169	199
C <sub>2</sub> -Naphthalene	156	<b>181</b>	197	199	171	<b>201</b>
C <sub>3</sub> -Indene	158	183	199	201	173	203
C <sub>1</sub> -Acenaphthylene	166	<b>191</b>	207	209	181	<b>211</b>
C <sub>1</sub> -Biphenyl	168	193	<b>209</b>	211	183	213
C <sub>3</sub> -Naphthalene	170	<b>195</b>	211	213	<b>185</b>	<b>215</b>
Phenanthrene	178	<b>203</b>	<b>219</b>	221	193	223
C <sub>2</sub> -Acenaphthylene	180	<b>205</b>	221	223	<b>195</b>	225
C <sub>2</sub> -Biphenyl	182	207	<b>223</b>	225	197	227
C <sub>1</sub> -Phenanthrene	192	<b>217</b>	233	235	207	237
C <sub>3</sub> -Acenaphthylene	194	<b>219</b>	235	237	209	239
C <sub>3</sub> -Biphenyl	196	<b>221</b>	237	239	211	241
Pyrene	202	227	<b>243</b>	<b>245</b>	217	247
C <sub>2</sub> -Phenanthrene	206	<b>231</b>	247	249	221	251
C <sub>1</sub> -Pyrene	216	241	257	259	<b>231</b>	261
C <sub>3</sub> -Phenanthrene	220	<b>245</b>	261	263	235	265
C <sub>2</sub> -Pyrene	230	255	271	273	<b>245</b>	275
C <sub>3</sub> -Pyrene	244	269	285	287	259	289

<sup>a,b</sup>Consideration of 1°, 2° and 3° amides and amines is implicit as {Ar-(CH<sub>2</sub>)<sub>2</sub>-CONH<sub>2</sub>, Ar-CH<sub>2</sub>-CONH(CH<sub>3</sub>), and Ar-CON(CH<sub>3</sub>)<sub>2</sub>} and {Ar-(CH<sub>2</sub>)<sub>2</sub>-NH<sub>2</sub>, Ar-CH<sub>2</sub>-NH(CH<sub>3</sub>), and Ar-N(CH<sub>3</sub>)<sub>2</sub>} are both sets of structural isomers and so are isobaric.

the monopropellant attitude adjustment thrusters; and (3) volatile organics introduced into the sample return capsule during atmospheric reentry as a consequence of pressure re-equilibration. To provide a measure of the contamination from these sources, an aerogel witness coupon, WCARM11CPN, was attached to the arm of the aerogel sample tray assembly. During the comet encounter, its location meant that it was screened from the gas/dust flux by the spacecraft's Whipple shield, but was otherwise exposed to everything else that the aerogel in the sample collection tray encountered.

Samples from the witness coupon were analyzed by ultra-L<sup>2</sup>MS, see Table 1. Under “normal” operating conditions, no organic species were observed above instrumental background levels. The term normal is taken in this context to mean the same conditions as those used for the analysis of the cometary aerogel tracks discussed previously. This does not imply that the aerogel is free of contamination, but rather it does not rise to a level that would perturb or alter the “cometary” organic signature recorded in the aerogel impact tracks. This

said, such a statement must also be tempered by the possibility that under the extreme physical conditions produced in an impact, some residual carbonaceous material originally present in the aerogel but not detectable by L<sup>2</sup>MS could be thermally processed into organic alteration products, which are observable by L<sup>2</sup>MS (Spencer and Zare 2007).

### Aluminum Oxide Shots into Blank Aerogel

As part of an ongoing investigation of potential contamination artifacts, the effect of firing inert particles into blank aerogel was investigated. These experiments were aimed at addressing two issues critical to interpreting the organic spectra obtained from Stardust samples, specifically,

- The potential for contamination of the impact particle by residual organic species present with the original aerogel.
- The possibility of thermal alteration of residual organics in the aerogel at, or adjacent to, a captured particle as a consequence of the impact thermal pulse.

Using the 5 m light-gas gun in the JSC Experimental Impact Laboratory, aluminum oxide ( $\text{Al}_2\text{O}_3$ ) particles 60  $\mu\text{m}$  in diameter were shot at approximately  $6.1 \text{ km s}^{-1}$  into a blank aerogel sample; simulating the conditions of Stardust collection. Figure 7 (upper image) shows a small rectangular cross section (approximately 3 mm thick) removed from the postshot aerogel with numerous impact features present. From this section, an individual track was exposed by splitting it open along its length using a stainless steel surgical scalpel, Fig. 7 (lower image) shows the lower half of the exposed track. Spectra were obtained by  $\mu\text{L}^2\text{MS}$  along the impact track and in the surrounding aerogel. Figure 8 shows three sets of mass spectra obtained from just below entrance hole into the aerogel labeled “Track Entrance,” approximately 4.5 mm down the track from the point of entry labeled “Down Track,” and in a proximate region of surrounding aerogel that was visual free of tracks labeled “Off Track.”

The mass spectrum obtained “Off Track” in aerogel (which was not from Stardust flight spares), shows a large residual organic background including naphthalene, phenanthrene, pyrene, and their associated alkylation series. Such organic contaminants are an inevitable consequence of aerogel synthesis, which is addressed further in the Discussion section. The presence of  $\text{Al}^+$  and  $\text{Al}_2\text{O}^+$  in the spectrum indicates that while the analyzed area was visually devoid of large tracks, it was nevertheless penetrated by microscopic  $\text{Al}_2\text{O}_3$  fragments. This said, for the purpose of comparison, we will assume that the “Off Track” spectrum is broadly representative of the baseline aerogel background. Relative to this aerogel background, the mass spectrum obtained at the “Track Entrance,” indicates a substantial reduction of about 30-fold in the abundance of organic species. We postulate this reduction likely arises from two factors: the first is simply due to the reduction in surface area of the compressed aerogel forming the track bulb; and the second is by shock induced thermal pyrolysis. In effect, the thermal pulse produced by impacting particle destroys those organics present in the aerogel in the chemical equivalent of sterilization. This interpretation is supported by the gradual reappearance of the background organic signature when descending down the track from the point of entry. This correlates with the decreasing temperature produced by impact heating as the particles velocity is gradually attenuated by passage through the aerogel. At a distance of about 4.5 mm from the initial point of impact, the overall organic signature is reduced only about 4-fold. More significant, however, is the appearance of a secondary higher mass envelope in the “Down Track” spectrum, which is characteristic of the free radical polymerization of PAHs presumably initiated by the thermolytic cleavage

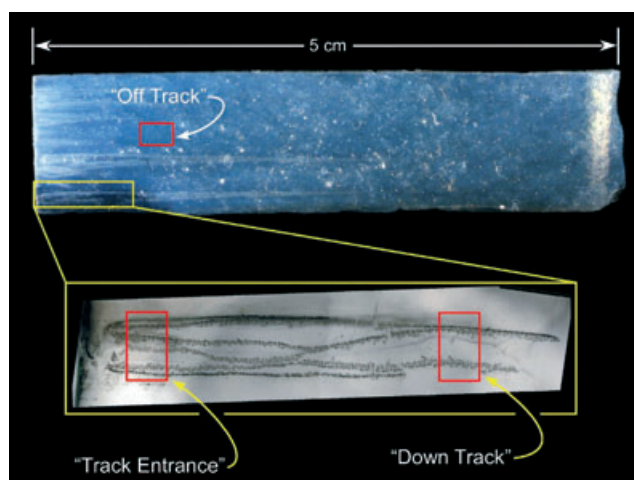
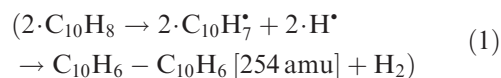
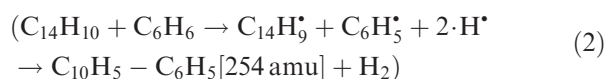


Fig. 7. Optical image of a 3 mm thick slice from an aerogel block (not Stardust flight spare aerogel) shot with 60  $\mu\text{m}$   $\text{Al}_2\text{O}_3$  particles at  $6.1 \text{ km s}^{-1}$  using the JSC Light Gas Gun Facility. The impacting particle vector is from left to right and numerous carrot shaped impact tracks are visible. The lower image shows an exploded view of the upper portion an individual track that was split open along its length using a stainless steel surgical scalpel. Two regions along this exposed track were analyzed by  $\mu\text{L}^2\text{MS}$  and are indicated by the red boxes labeled “Track Entrance” and “Down Track.” A third region labeled “Off Track” in the upper image was also analyzed as baseline comparison and corresponds to an area visually free of tracks.

of C–H bonds. Hence, the presence of the peak at 254 amu can arise from the condensation of two naphthalene radicals



or a phenanthrene and benzene radical



As with the primary mass envelope, this secondary mass envelope shows a primary alkylation series. This suggests that as the impact shock temperature decreases down the track, the complete pyrolysis of organics indigenous to the aerogel is gradually superseded by incomplete pyrolysis and subsequent free radical polymerization. At the end of the track defined by the terminal particle (spectrum not shown), no alteration or diminution of the aerogel background is seen, as expected.

## ANALYSIS

From the spectra present in Figs. 5 and 6, it is clear that there is an organic matter associated with cometary impact features. Nevertheless, caution is warranted when interpreting these results. The observation of organic

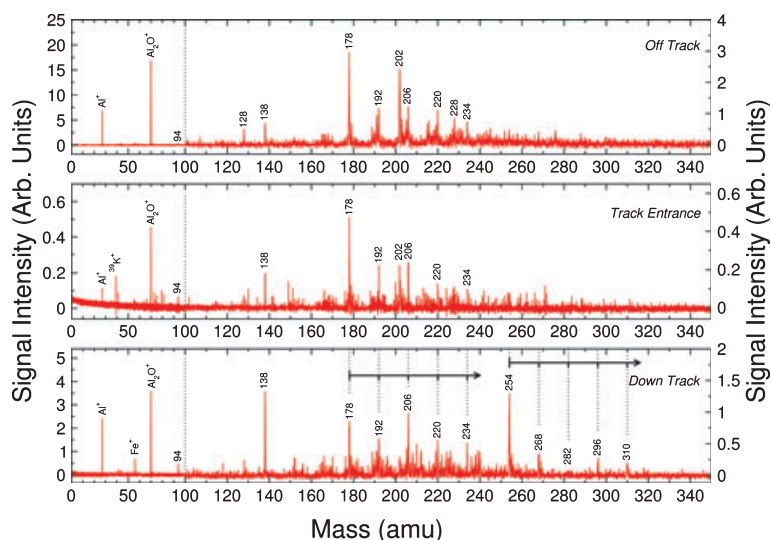


Fig. 8.  $\mu$ ltra- $L^2$ MS spectra obtained from the three analysis regions indicated in Fig. 7. Prominent peaks are mass indexed and represent simple 2–4 fused ring PAHs and their alkylated homologs—specifically peaks series at 178, 192, 206, 220, and 234 amu corresponding to phenanthrene and its alkylated homologs, while peaks at 128, 202, and 228 amu represent naphthalene, pyrene, and chrysene, respectively. In the “Down Track” trace, the secondary mass envelope consistent with thermal polymerization is defined by the peak sequence 254, 268, 282, 296, 310 amu.

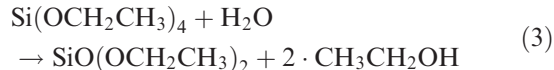
molecules present in particulate matter extracted from Stardust aerogels does not necessarily imply that those exact same molecules were present on comet 81P/Wild 2. At least five factors could potentially influence the nature and distribution of the organic species observed. In no particular order, these are

- Aerogel by its very nature inevitably incorporates organic contaminants during its manufacture, which are subsequently difficult, if not impossible, to remove completely.
- Particles collected by the Stardust spacecraft spent between 20 min and 1 h in the comet’s coma exposed to the ambient solar radiation field.
- Hypervelocity capture of particles into aerogel converts a considerable fraction of a captured particle’s translational and angular kinetic energy into heat that could have pyrolyzed or otherwise altered the original organics.
- Cometary organics may be highly reactive under normal ambient conditions, particularly with respect to hydrolysis.
- The high intrinsic internal surface area of aerogel combined with the propensity of silica surfaces, in general, to adsorb organic species makes aerogel highly susceptible to terrestrial contamination both during curation and/or analysis.

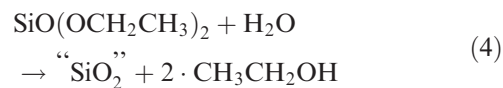
### Intrinsic Aerogel Purity

Silica aerogels for Stardust (Hrubesh 1989; Jones 2000;] were produced via the two step “sol-gel” process.

The first step involves the catalytic hydrolysis of tetraethylorthosilicate ( $\text{Si}(\text{OCH}_2\text{CH}_3)_4$ ) to produce a distribution of hydrolyzed diethoxy monomers (Brinker et al. 1982).



In the second step, addition of more water allows the hydrolysis reaction to go to completion resulting in the condensation of the oligomeric and monomeric species formed during the first step. The product is a highly porous 3-dimensional silicon dioxide solid phase (i.e., the aerogel) filled with ethanol.



The microstructure of the aerogel is determined by the relative rates of the hydrolysis and condensation reactions. The ethanol by-product is then removed by a combination of drying and dilution with acetonitrile ( $\text{CH}_3\text{CN}$ ). Although silica aerogels can be manufactured with high purity in regard to inorganic elements (Flynn and Sutton 1990), this is not the case for organics. Organic contamination to some degree is inevitable due to a combination of incomplete hydrolysis of the reactants, secondary side-reactions, incomplete removal of solvent residuals and the inherent “stickiness” of silica aerogels toward organic species. As early as 1990, Hartmetz et al. (1990a, 1990b) recognized that the

presence of significant amounts of hydrocarbon contaminants in aerogels could present a problem in their use as a collection medium for cosmic dust. In their studies of 0.06 and 0.12 g cm<sup>-3</sup> silica aerogels that were at the time under consideration as an IDP collection medium, they reported the presence of significant quantities of volatile organic contaminants, which they attributed to unreacted precursor tetramethoxysilane (Si(OCH<sub>3</sub>)<sub>4</sub>) and associated solvents used during synthesis. Although the degree of volatile contamination could be reduced by as much as approximately 50% by heating in a vacuum at 250 °C for 72 h, it could not be completely removed. Several years later, Huang et al. (1993) investigated the removal of carbonaceous contaminants from aerogel using variety of preconditioning procedures. Solvent extraction and/or heating at 500 and 700 °C in both air and under vacuum were noted to be largely ineffective. They determined that the most effective way to remove carbonaceous contaminants was by supercritical extraction with CO<sub>2</sub>, which could reduce their levels up to an order of magnitude (Huang et al. 1994). This procedure was not, however, employed for the Stardust aerogels, which instead employed a two stage process involving first high temperature supercritical point extraction to remove excess acetonitrile (CH<sub>3</sub>CN) followed by heating to 300 °C for 72 h in a controlled flow of filtered air at 5–6 psi. (Tsou et al. 2003). This procedure removed the level of organic C present in the aerogel from approximately 2.4% to <0.5% by mass, with the residual organics chiefly in the form of aliphatic –CH<sub>2</sub>– and –CH<sub>3</sub> groups (Tsou et al. 2003).

### Solar Radiation Processing

The Stardust mission did not directly sample the surface of a comet. Rather it collected dust particles originating from source locations below the comet surface that were ejected into the comet coma from two out gassing jets (Brownlee et al. 2006). Once ejected from the comet, these particles are estimated to have spent between 20 min and several hours in the coma prior to collection and during this time were subject to the ambient solar UV flux. At 1 AU, this solar flux is approximately 1366 W m<sup>-2</sup> (SOLAR2000; Tobiska 2004), so at the distance of 1.86 AU from the Sun where collection occurred, the nominal solar photon flux would have been on the order of approximately 400 W m<sup>-2</sup> (i.e., 1366/(1.86)<sup>2</sup>). The UV component of this flux can act both directly and indirectly with any organic matter within these dust particles. In the gas phase, photodissociation and ionization of sublimed ices initiates a complex cascade of ion-molecule and radical

reactions creating a dynamic chemically active coma environment. The most important reaction in this context is the photodissociation of H<sub>2</sub>O, to generate hydroxyl radicals (H<sub>2</sub>O → H· + OH·), which can undergo rapid abstraction and addition reactions with aromatic hydrocarbons. In addition, aromatic moieties are themselves also susceptible to photodecomposition as most PAHs have relatively large UV adsorption cross sections. For example, benzene (C<sub>6</sub>H<sub>6</sub>), the simplest and most volatile PAH in the gas phase, has an estimated rate constant for photodestruction of approximately 1.1 × 10<sup>3</sup> s<sup>-1</sup> at 1 AU. (Crovisier 1994). The mechanism proceeds via initial dissociation to either the phenyl (C<sub>6</sub>H<sub>5</sub>·) or benzyne (C<sub>6</sub>H<sub>4</sub>·) radical, which upon further photolysis, leads to various C<sub>3</sub> bearing species. Indeed, the observation of the cyclopropenyl ion (C<sub>3</sub>H<sub>3</sub><sup>+</sup>) in the extended coma of Halley has been attributed to either unsaturated hydrocarbon chains (C<sub>n</sub>H<sub>2n-3</sub><sup>+</sup> series) or aromatic precursors (Korth et al. 1989, 1990). Modeling studies suggest that for larger PAHs, the photodestruction rate decreases with size so that at a heliocentric distance of 1.86 AU (i.e., that at which Stardust collection occurred), the half-life (*t*<sub>1/2</sub>) for phenanthrene (C<sub>14</sub>H<sub>10</sub>) is on the order of approximately 100 s, while that for ovalene (C<sub>32</sub>H<sub>14</sub>) is only approximately 3 s (Joblin et al. 1997). This decrease in stability arises because as the size of the fused ring PAH increases, the rate of UV adsorption becomes proportionally larger than the rate of radiative relaxation by fluorescence and phosphorescence. While these processes related to gas phase species, it is not necessary for a given PAH to enter the gas phase in order to be susceptible to UV photolysis reactions. Most of the cometary dust particles sampled by Stardust spacecraft were in the micron to submicron size range (Kearsley et al. 2008). If, for lack of a better assumption, we assume the optical penetration length of UV photons into dust particles is on the order of the wavelength of the photon, then a significant fraction of a grains involatile organic inventory could be susceptible to photolytic reactions.

### CYROGENIC CHEMISTRY

A primary mechanism for the evolution of organic matter in interstellar and hence cometary environments is through radiolysis of icy grain mantles by Lyman-α radiation (121.6 nm) and cosmic rays, which leads to the formation of radical species and ions. These molecular fragments can, assisted by transient heating events (e.g., shock waves), undergo solid state diffusion and recombination reactions to yield new molecular species (e.g., Bernstein et al. 1995). In the case of the comet 81P/Wild 2 particles, any ice grain mantles they may have had at ejection would have rapidly sublimed

( $T > 200$  K) away in the cometary coma prior to collection, possibly leaving behind a chemically reactive organic residue. Impact heating associated with capture in aerogel and hydrolysis by  $\text{H}_2\text{O}$  vapor during curation would then act to alter the original organic inventory.

### Impact Thermal Alteration

During the capture of a particle through hypervelocity impact, a substantial fraction of the particle's kinetic energy will be released as thermal radiation resulting in a large transient temperature pulse. The kinetic energy release for a simple impactor is simply the sum of the translational and rotational energies. Particle rotation can occur either through collision or by radiation torque; the latter arises from the anisotropic scattering of solar photons. Laboratory studies of interstellar dust grain analogs levitated in an electrodynamic balance and irradiated by laser irradiation (Abbas et al. 2004) suggest that the Stardust particles could not have achieved rotational frequencies much higher than a few thousand Hertz from radiation torque alone. Under these conditions, the kinetic energy of a particle impacting aerogel at  $6.1 \text{ km s}^{-1}$  is dominated by the linear kinetic energy term. For a spherical particle of radius  $r$ , density  $\rho$ , and impact velocity  $v$ , the kinetic energy released will then be:

$$E_{\text{kinetic}} = \frac{2}{3} \cdot \pi \cdot r^3 \cdot \rho \cdot v^2 \quad (5)$$

This can be compared with the energy required to vaporize the particle which can be approximated<sup>3</sup> as:

$$E_{\text{vaporization}} = \frac{4}{3} \frac{\pi \cdot r^3 \cdot \rho}{M.W.} \left( \Delta H_{\text{fusion}} + \Delta H_{\text{evaporation}} + \int_{T_{\text{nominal}}}^{T_{\text{melt}}} C_p \cdot dT \right) \quad (6)$$

where  $C_p$  is the specific heat capacity,  $T_{\text{melt}}$  is the melting temperature,  $T_{\text{nominal}}$ <sup>4</sup> is the starting ambient

<sup>3</sup>For the sake of simplicity, pressure shock functions that will affect such a rapid phase change and expansion are neglected. Furthermore, we assume that the vaporization energy can be calculated solely on the basis of the particle's composition dependent latent heat of evaporation.

<sup>4</sup>If we assume a particle to be a perfect spherical blackbody in thermal equilibrium with itself and which adsorbs all the solar energy it intercepts, the nominal temperature is approximately given by

$$T_{\text{nominal}} = T_{\text{sun}} \sqrt{\frac{r_{\text{sun}}}{2d}}$$

where  $T_{\text{sun}}$  is the surface temperature of the Sun (approximately 5780 K),  $r$  is the radius of the Sun (approximately  $6.96 \times 10^8$  m) and  $d$  is the distance from the Sun (1.86 AU approximately  $2.78 \times 10^{11}$  m). This gives a value of  $T_{\text{nominal}}$  approximately 200 K.

Table 3. Kinetic versus vaporization energies for organic and inorganic particles  $10 \mu\text{m}$  in diameter traveling at  $6.1 \text{ km s}^{-1}$ .

Particle composition	Kinetic energy (mJ)	Vaporization energy (mJ)	Ratio
Coronene ( $\text{C}_{24}\text{H}_{12}$ )	0.01000	0.00059	16.9
Quartz ( $\text{SiO}_2$ )	0.02580	0.03120	0.8

temperature,  $\Delta H_{\text{fusion}}$  is the enthalpy of fusion,  $\Delta H_{\text{evaporation}}$  is the enthalpy of evaporation, and  $M.W.$  is the molecular weight. Representative values of the kinetic energies and vaporization energies are shown in Table 3 for organic and inorganic particles  $10 \mu\text{m}$  in diameter having an impact velocity of  $6.1 \text{ km s}^{-1}$ .

For inorganic particles, the kinetic energy released during impact is on the order of the energy required to vaporize the particle, while for organic particles, the kinetic energy typically exceeds the vaporization energy by an order of magnitude. Clearly while these calculations are gross simplifications, and only a fraction of the impact kinetic energy will actually go to heating the particle itself, it nevertheless illustrates that the effects of impact heating cannot be ignored and will affect to a greater or lesser degree the nature of the cometary organics preserved with tracks.

In general, when complex organic matter is heated to high temperatures or sputtered by fast ions or energetic photons, small molecular fragments and atoms are lost from the material (such as H, O,  $\text{H}_2$ ,  $\text{O}_2$ , OH,  $\text{H}_2\text{O}$ , CO,  $\text{CO}_2$ , CN, and  $\text{CH}_4$ ) in a process called carbonization (Fristrom 1995; Jenniskens et al. 2004). Further heating (up to approximately 700 K) leads to additional loss of H and  $\text{H}_2$  in a process of polymerization, which is accompanied by the growth of aromatic ring structures. Prolonged heating in a confined environment leads to graphitization, which is the stacking of those rings into layers to form a crystal (e.g., Koidl et al. 1989). Further temperature increase leads to decomposition by loss of  $\text{H}_2$ , CN, CH,  $\text{C}_2$ , HCN,  $\text{NH}_3$ , and  $\text{C}_2\text{H}$ . In the absence of rapid radiative cooling, the latter stage of decomposition hydrocarbon radicals higher than  $\text{C}_2$  rapidly undergo fission into lower molecular weight products, leaving only the thermally stable single- and double-bonded C radicals. Carbon atoms are also present, but at low abundance due to thermodynamic factors (Fristrom 1995; Rairden et al. 2000). Upon cooling, these lower molecular weight products can recondense into amorphous C to form soot. In the case of impact thermal alteration, the effects are likely to be less well defined because of the short duration (about  $\mu\text{s}$ ) of the thermal event. For thermally activated unimolecular decomposition reactions (i.e.,  $\text{A} \rightarrow \text{B} + \text{C} + \dots$ ) the reaction

kinetics follows Arrhenius behavior so that the rate of reaction only has a linear dependence with time but an exponential dependence with temperature. Hence, for a rapid thermal pulse, the reaction products will be defined purely by kinetics, while for slower thermal processes, thermodynamic control will begin to exert influence over reaction products.

### Aerogel Surface Adsorption

Silica aerogels are particularly prone to contamination by volatile organic species because of the surface adsorption properties of SiO<sub>2</sub> surfaces. The ability of silica to readily adsorb polar organic species is particularly well known to the semiconductor industry where trace volatile organic contamination from polymeric construction materials can ruin wafer fabrication (Sago and Hattori 1996). In the case of silica aerogels, this effect is further compounded by their high (density dependent) surface area. For a typical 100 mg cm<sup>-3</sup> silica aerogel, the surface area (as determined by nitrogen adsorption/desorption) is on the order of 600–1000 m<sup>2</sup> g<sup>-1</sup>. As the Stardust cometary aerogel tiles have densities of between 5 mg cm<sup>-3</sup> at the exposed surface and increasing to 50 mg cm<sup>-3</sup> at the base, we can expect 1000 m<sup>2</sup> g<sup>-1</sup> to represent a lower limit. For common pollutants such as chlorobenzene or trichloroethylene, silica aerogels absorb 130 times the quantity of chemicals gram-for-gram than granulated activated carbon (GAC) (Lerner 2004).

## DISCUSSION

### A Cometary Origin to Organic Material in Stardust Tracks?

Given the intrinsic properties of silica aerogels and the effects of hypervelocity capture, it is inevitable that terrestrial contamination concerns will always need to be considered in interpreting results from the organic analysis of Stardust aerogels. Nonetheless, we feel that a good argument can be made to support our contention that many of the organic compounds observed in the mass spectra from cometary tracks C2115 Track 22 and FC-12-2-16 Fragment 12A-3 are not artifacts of terrestrial contamination.

Analysis of flight aerogel coupons WCARM11CPN,0,10 and WCARM11CPN,0,11, which were not exposed to the 81P/Wild 2 particle flux, showed a remarkably small organic background, at least two orders of magnitude below the integrated signal from either of the cometary tracks. It is likely that the two periods during which the aerogel collection tray was deployed for interstellar collection prior to comet

encounter, collectively amounting to 195 days (Feb–May 2000, Orbit 1 and Aug–Dec 2002, Orbit 2), allowed the extensive degassing and/or sublimation of residual organic contaminants from the aerogel. In effect, the Stardust aerogel was likely cleaner just prior to the collection of comet dust than it was when it was manufactured and launched.

The analysis of tracks produced by aluminum oxide spheres fired into aerogel at the same relative velocity as the Stardust comet encounter demonstrates that there is minimal organic contamination of the upper walls of the impact track by either the organics inherently present in the aerogel and/or their thermal alteration products. As this is where the highest concentration of organics was identified for both cometary tracks, it implies that they derived from a source other than contaminants in the aerogel. Furthermore, many of these organic species (e.g., naphthalene and phenanthrene) would have rapidly sublimated under vacuum conditions if they were simply surface adsorbates. This suggests that they are likely associated with fragments of the impactor particle that were shed and embedded into the track wall during impact (perhaps bound to heavier molecular weight kerogen-like refractory material and/or trapped within a mineral matrix).

### Thermal Alteration Effects during Capture?

Independent of the results reported here, there is unequivocal evidence, in at least some instances, that refractory organic matter associated with the cometary particles collected by Stardust was preserved despite the effects of hypervelocity capture. This is in the form of modest D and <sup>15</sup>N enrichments that have been reported from ion microprobe studies of terminal particles mechanically extracted from Stardust aerogel tracks (McKeegan et al. 2006; Sandford et al. 2006). In all cases, the D enrichments were both heterogeneously distributed and correlated with C abundance, implying the carrier to be organic in nature. However, the abundance and magnitude of the D fractionation is not as large as that which might be anticipated given the low temperature interstellar/protostellar heritage associated with comets. One way to dilute isotopic enrichments is through the partial pyrolysis of the organic carrier phase during impact induced shock heating. For example, Mimura et al. (2007) recently demonstrated the selective release of deuterium from Murchison (CM2) insoluble organic matter by shock impact. This illustrates the fundamental point that all cometary particles collected by Stardust will have experienced a significant thermal pulse during impact. The consequences of this on any indigenous organic matter will be a combination of three outcomes.

1. Survival without alteration.
2. Partial to complete thermal alteration and/or decomposition.
3. Impact synthesis of new organics species.

The extent to which each outcome contributes to the total sample is a sensitive function of a diverse range of physical parameters including the nature, composition, and size of the impacting particle. Consequently, it may never be possible to fully deconvolve the effects of thermal impact alteration on the organic matter observed in Stardust tracks. This being said, the types of aromatic organic species we have observed are considered relatively thermally stable and are likely to be among the most resistant to impact alteration. Bunch et al. (Bunch et al. 1993, 1995) investigated the survival of PAHs in particles of Murchison (CM2) matrix fired at 4.8 and 5.9 km s<sup>-1</sup> in to an Al plate. While both low and high mass PAHs were largely destroyed on impact, they determined that intermediate mass PAHs (202–220 amu) remained largely unaffected.

### Comparisons with Carbonaceous Chondrites and Interplanetary Dust Particles

An overview comparison of the organic material recorded in the two Stardust aerogel tracks with a representative selection of L<sup>2</sup>MS spectra acquired from both carbonaceous chondrites and stratospheric interplanetary dust particles (IDPs) is shown in Fig. 9. The organic material present in the two Stardust aerogel tracks can be interpreted as the overlay of two groupings of organic molecules. In the first group are the simple fused PAH species such as naphthalene (128 amu), phenanthrene (178 amu), pyrene (202 amu), chrysene (228 amu) benzopyrene (252 amu), and pentacene (278), as well as their associated alkylation series derived from successive addition of methylene (–CH<sub>2</sub>–) subunits. These molecules give rise to the even mass parent molecular ions in the L<sup>2</sup>MS spectra. The distribution of these species is broadly similar to the spectra observed from relatively unaltered carbonaceous chondrites. Indeed, carbonaceous chondrites and comets may well share a common heritage as many theoretical and observational analyses suggests that many comets will eventually evolve into asteroids, and several extinct cometary nuclei are already suspected to be represented in the near-Earth object population (Lodders and Osborne 1999).

The second group represents the N bearing aromatic species responsible for the prominent odd mass molecular ions observed in the L<sup>2</sup>MS spectra, and which are not observed in the spectra of carbonaceous chondrites. Detailed analysis of the spectra suggests that

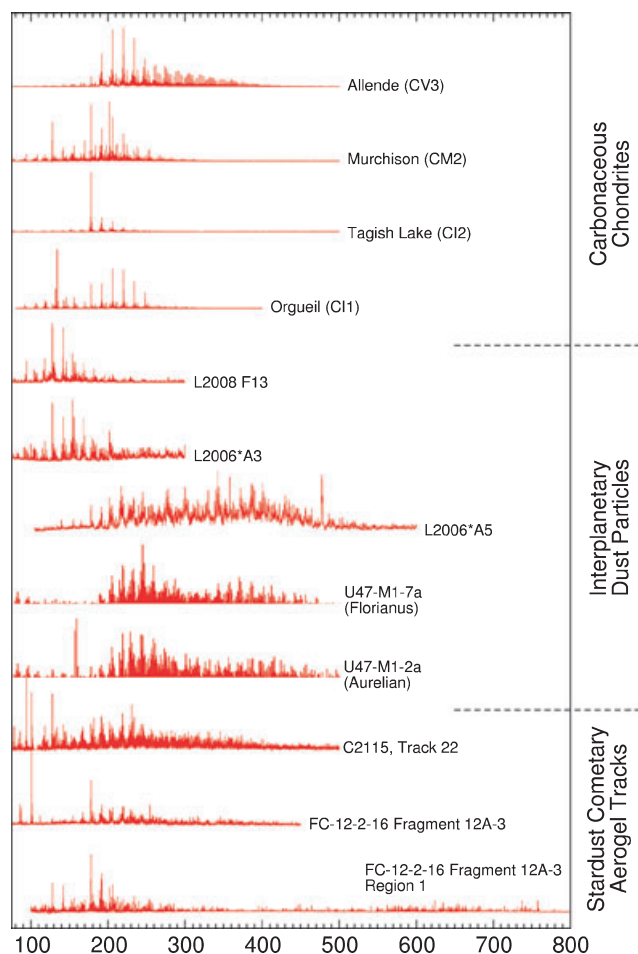


Fig. 9. Overview of the  $\mu$ L<sup>2</sup>MS spectra obtained from the two Stardust aerogel samples compared with those obtained from the matrix of four carbonaceous chondrites and five individual stratospheric interplanetary dust particles (IDPs). Carbonaceous chondrites generally show simple mass spectra consistent with 2–6 ring aromatic hydrocarbons and associated alkylation series with an overall mass envelope that tends to increase in both size and position in correlation with the degree of thermal metamorphism experienced by the chondrite. By contrast, IDPs show highly variable mass spectra suggesting a more diverse range of organic species and in the case of L2006\*A5, U47-M1-7a, and U47-M1-2a, they also demonstrate a preponderance of odd mass aromatic species.

the most consistent assignment for the odd mass peaks is to the molecular ions of aromatic nitriles of the general form Ar–(CH<sub>2</sub>)<sub>n</sub>–CN. In this respect it is interesting to note that, although plagued by the poor impact ionization yield due to the relatively low encounter velocity, the Cometary and Interstellar Dust Analyzer (CIDA) flown onboard the Stardust spacecraft was able to acquire 29 particle spectra during the flyby of comet 81P/Wild 2 (Kissel et al. 2004, 2005). All but one of these spectra implied that the impacting particles

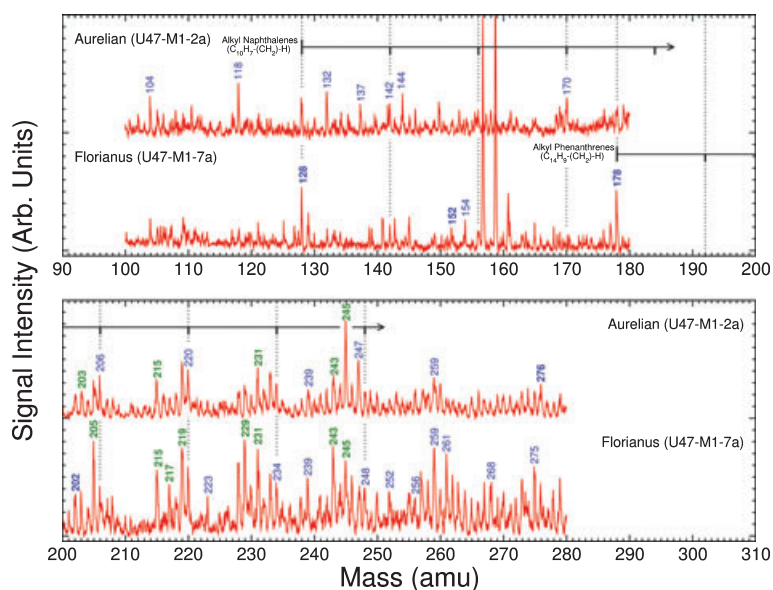


Fig. 10. Expanded ultra- $L^2$ MS spectra for two stratospheric interplanetary dust particles U47-M1-7a and U47-M1-2a, which show similarities to the Stardust spectra illustrated in Figs. 5 and 6. Prominent peaks are mass indexed using the labeling scheme described for Fig. 5, and the positions of the naphthalene and phenanthrene alkylation series are indicated. The absence of spectra coverage in the mass windows 90–100, 180–200, and 280–310 amu is due to truncation of the original archived raw data sets.

were carbonaceous in nature and were N rich. In fact, the dominant negative ion (excluding  $H^-$  and  $e^-$ ) measured in these mass spectra was  $CN^-$ .

The only other extraterrestrial samples analyzed using the  $L^2$ MS technique that have also, in specific instances, exhibited a similar distribution of odd mass organic species are stratospherically collected interplanetary dust particles (IDPs) (Clemett et al. 1993). While generally the organic composition of IDPs, as measured by the  $L^2$ MS technique, show large variations in both absolute and relative abundances from particle to particle, in several instances, prominent odd mass peak distributions mirroring those observed in Stardust aerogel tracks have been observed. Figure 10 illustrates the expanded spectra acquired from two chondritic cluster IDPs, Aurelian (U47-M1-2a) and Florianus (U47-M1-7a), both of which also demonstrated significant bulk isotopic anomalies (Aurelian  $\delta D = 771 \pm 85\%$ ; Florianus  $\delta D = 1120 \pm 85\%$  and  $\delta^{15}N = 411 \pm 20\%$ ). Interestingly, ion microprobe measurements of other fragments of these same particles showed high  $CN^-/C^-$  ion ratios of about 1.2 for Aurelian and about 3.2 for Florianus. The presence of the dominant odd mass peaks in these spectra were also interpreted to be due to the presence of a N containing functionality attached to a PAH parent. At that time, the nature of the N containing functionality was thought to be either a nitrile ( $-C\equiv N$ ) or an amine ( $-NH_2$ ). Speciation of N in IDPs has also been investigated by electron energy loss spectroscopy (EELS). Keller et al. (1997) used EELS to study the N

k-edge in the  $^{15}N$  enriched IDP L2011R11. Comparison with various N standards also lead to the interpretation of an organic carrier phase having either amide ( $-NH_2$ ) and/or nitrile ( $-C\equiv N$ ) functionality. The similarity between the organic matter associated with Stardust aerogel tracks and that present in some IDPs is consistent with the widely held, but difficult to prove unambiguously, interpretation that a fraction of IDPs (estimates range from approximately 10 to 50%) are derived from cometary sources.

### Significance

The presence of aromatic nitriles in both IDPs and Stardust samples from comet 81P/Wild 2 is likely to be of interest to both the astrobiology and remote sensing communities.

- Cometary dust is considered to have provided a significant contribution to the prebiotic organic inventory of the early Earth (e.g., Levasseur-Regourd and Desvoivres 2004; Meech and Bauer 2004; Krueger and Kissel 2006; Thomas et al. 2006). The presence of N containing organic species in comet dust is of particular importance in this respect. On the early abiotic Earth (and Mars), the production of N bearing organics is expected to have been extremely slow and difficult in the absence of biology. The dominant form of N on the Earth in the Hadean period (4.6–3.8 Ga) is believed to have been  $N_2$  (produced by volcanic outgassing), so any reaction sequence resulting in the formation

of N containing organics would require cleavage of the N≡N triple bond, one of the strongest chemical bonds known ( $\Delta H_{\text{dissociation}} = 944.7 \text{ kJ mol}^{-1}$ ). This bottle neck in the production of organo-N compounds, considered a prerequisite to the genesis of life, can be circumvented if these species were instead exogenously acquired from comets.

- As noted earlier, molecules released from the comet are immediately exposed to solar radiation and are subject to photodissociation and fast ion-neutral reactions (Combi et al. 2004). Some species, for example H<sub>2</sub>O, show spatial distributions that suggest they are primary ice components, i.e., they were released directly from the comet nucleus. Others, like CN\* are more complex. At heliocentric distances larger than approximately 3 AU, the production rate of CN\* can be accounted for by the UV photolysis of HCN released by the sublimation of primary ices. Closer to the Sun, however, at distances less than approximately 3 AU, the formation of an extended CN\* distribution requires the presence of an additional CN<sup>-</sup> containing molecular carrier species (Mumma et al. 1993; Strazzulla 1999; Bockelee-Morvan et al. 2004). One hypothesis is the direct production of CN\* radicals by the photo or thermal degradation of complex refractory organic compounds present on cometary grains (Fraya et al. 2005). Aromatic nitriles of the type reported here from comet 81P/Wild 2 samples might be candidates and could also help to explain the known discrepancy in <sup>14</sup>N/<sup>15</sup>N isotope ratios observed between CN\* and HCN in some comets.

## CONCLUSIONS

The successful return of samples from comet 81P/Wild 2 by the Stardust spacecraft has provided a unique opportunity to investigate the nature and distribution of organic matter in cometary dust particles. Analysis of individual cometary impact tracks in silica aerogel reveals the presence of complex N rich aromatic organic matter. Directly attributing such matter to a cometary origin is complicated by both the significant potential for terrestrial contamination from the aerogel capture medium and the variable effects of thermal alteration inevitable in hypervelocity capture. Nevertheless experimental analysis of blanks and contamination checks leads us to conclude that many of the organic species observed in two cometary aerogel impact tracks are indigenous to the impact particle and are hence of cometary origin. However, it is likely that these species represent a variable mixture of what might be termed primary cometary organics present prior to

aerogel capture, and secondary cometary organics produced through impact alteration of these primary parent species.

Although there are some commonalities in the nature and abundance of the observed organic species to those present in the matrices of carbonaceous chondrites, they do differ significantly from one another. Most notably, the aromatic fraction of the organic matter associated with the Stardust cometary impact tracks appears to be N-rich, with the N functionality occurring predominantly in the form of aromatic nitriles (R-C≡N). We cannot yet exclude the possibility that the abundance of these aromatic nitriles has been influenced by impact thermal alteration of a precursor chondritic macromolecular material, as aromatic nitriles have been observed in pyrolysis studies of carbonaceous chondrites (Pearson et al. 2006). That said, the closest match to the organic matter from Stardust cometary impact tracks is found with stratospherically collected interplanetary dust particles, some of which also show the presence of complex N-rich aromatic species. These findings are consistent with the long held notion that a fraction of interplanetary dust is of cometary origin. Such species may be associated with one of the classes of carrier “parent molecules” thought responsible for the extended distributions of CN<sup>-</sup> seen in many cometary comae, which at small heliocentric distances (e.g., <3 AU) cannot be explained by the HCN photolysis alone (Fraya et al. 2005). The presence of organic N rich species in comets may have wider implication in regard to astrobiology as comets are likely to have contributed to the prebiotic chemical inventory of habitable regions in the solar system including the Earth and Mars.

*Acknowledgment*—We are grateful to O. Clemett for fruitful discussions and advice, and for financial support from the National Aeronautics and Space Administration Cosmochemistry program.

*Editorial Handling*—Dr. Ian Franchi

## REFERENCES

- Abbas M. M., Craven P. D., Spann J. F., Tankosic D., LeClair A., Gallagher D. L., West E. A., Weingartner J. C., Witherow W. K., and Tielens A. G. G. M. 2004. Laboratory experiments on rotation and alignment of the analogs of interstellar dust grains by radiation. *The Astrophysical Journal* 614:781–795.
- Alexander C. M. O. D., Fogel M., Yabuta H., and Cody G. D. 2007. The origin and evolution of chondrites recorded in the elemental and isotopic compositions of their macromolecular organic matter. *Geochimica et Cosmochimica Acta* 71:4380–4403.

- Allamandola L. J., Tielens A. G. G. M., and Barker J. R. 1985. Polycyclic aromatic hydrocarbons and the unidentified infrared emission bands—Auto exhaust along the Milky Way. *The Astrophysical Journal* 290:L25–L28.
- Allamandola L. J., Hudgins D. M., and Sandford S. A. 1999. Modeling the unidentified infrared emission with combinations of polycyclic aromatic hydrocarbons. *The Astrophysical Journal* 511:L115–L119.
- Altwegg K., Ehrenfreund P., Geiss J., and Huebner W. 1999. *Composition and origin of cometary materials*. Dordrecht: Kluwer Academic Publishers.
- Bernstein M. P., Sandford S. A., Allamandola L. J., Chang S., and Scharberg M. A. 1995. Organic compounds produced by photolysis of realistic interstellar and cometary ice analogs containing methanol. *The Astrophysical Journal* 454:327–344.
- Bernstein M. P., Sandford S. A., Allamandola L. J., Gillette J. S. B., Clemett S. J., and Zare R. N. 1999. UV irradiation of polycyclic aromatic hydrocarbons in ices: Production of alcohols, quinones, and ethers. *Science* 283:1135–1138.
- Bleeker E. A. J., Van der Geest H. G., Kraak M. H. S., De Voogt P., and Admiraal W. 1998. Comparative ecotoxicity of NPAHs to larvae of the midge *Chironomus riparius*. *Aquatic Toxicology* 41:51–62.
- Bockelee-Morvan D., Brooke T. Y., and Crovisier J. 1995. On the origin of the 3.2 to 3.6-micron emission features in comets. *Icarus* 116:18–39.
- Bockelee-Morvan D., Crovisier J., Mumma M. J., and Weaver H. A. 2004. The composition of cometary volatiles. In *Comets II*, edited by Festou M. C., Keller H. U., and Weaver H. A. Tucson, AZ: The University of Arizona Press. pp. 391–423.
- Bockelee-Morvan D., Lis D. C., Wink J. E., Despois D., Crovisier J., Bachiller R., Benford D. J., Biver N., Colom P., Davies J. K., Gérard E., Germain B., Houde M., Mehringer D., Moreno R., Paubert G., Phillips T. G., and Rauer H. 2000. New molecules found in comet C/1995 O1 (Hale-Bopp). *Astronomy and Astrophysics* 353:1101–1114.
- Brinker C. J., Keefer K. D., Schaefer D. W., and Ashley C. S. 1982. Sol-gel transition in simple silicates. *Journal of Non-Crystalline Solids* 48:47–64.
- Brownlee D., Tsou P., Aléon J., Alexander C. M. O' D., Araki T., Bajt S., Baratta G. A., Bastien R., Bland P., Bleuet P., Borg J., Bradley J. P., Brearley A., Brenker F., Brennan S., Bridges J. C., Browning N. D., Brucato J. R., Bullock E., Burchell M. J., Busemann H., Butterworth A., Chaussidon M., Chevront A., Chi M., Cintala M. J., Clark B. C., Clemett S. J., Cody G., Colangeli L., Cooper G., Cordier P., Daghlian C., Dai Z., D'Hendecourt L., Djouadi Z., Dominguez G., Duxbury T., Dworkin J. P., Ebel D. S., Economou T. E., Fakra S., Fahey S. A. J., Fallon S., Ferrinib G., Ferroit T., Fleckenstein H., Floss C., Flynn G., Franchi I. A., Fries M., Gainsforth Z., Gallien J.-P., Genge M., Gilles M. K., Gillet P., Gilmour J., Glavin D. P., Gounelle M., Grady M. M., Graham G. A., Grant P. G., Green S. F., Grossemey F., Grossman L., Grossman J. N., Guan Y., Hagiya K., Harvey R., Heck P., Herzog G. F., Hoppe P., Hörz F., Huth J., Hutcheon I. D., Ignatyev K., Ishii H., Ito M., Jacob D., Jacobsen C., Jacobsen S., Jones S., Joswiak D., Jurewicz A., Kearsley A. T., Keller L. P., Khodja H., Kilcoyne A. L. D., Kissel J., Krot A., Langenhorst F., Lanzirotti A., Le L., Leshin L. A., Leitner J., Lemelle L., Leroux H., Liu M.-C., Luening K., Lyon I., MacPherson G., Marcus M. A., Marhas K., Marty B., Matrajt G., McKeegan K., Meibom A., Mennella V., Messenger K., Messenger S., Mikouchi T., Mostefaoui S., Nakamura T., Nakano T., Newville M., Nittler L. R., Ohnishi I., Ohsumi K., Okudaira K., Papanastassiou D. A., Palma R., Palumbo M. E., Pepin R. O., Perkins D., Perronnet M., Pianetta P., Rao W., Rietmeijer F. J. M., Robert F., Rost D., Rotundi A., Ryan R., Sandford S. A., Schwandt C. S., See T. H., Schlutter D., Sheffield-Parker J., Simionovici A., Simon S., Sitnitsky I., Snead C. J., Spencer M. K., Stadermann F. J., Steele A., Stephan T., Stroud R., Susini J., Sutton S. R., Suzuki Y., Taheri M., Taylor S., Teslich N., Tomeoka K., Tomioka N., Toppani A., Trigo-Rodríguez J. M., Troadec D., Tsuchiyama A., Tuzzolino A. J., Tylliszczak T., Uesugi K., Velbel M., Vellenga J., Vicenzi E., Vincze L., Warren J., Weber I., Weisberg M., Westphal A. J., Wirick S., Wooden D., Wopenka B., Wozniakiewicz P., Wright I., Yabuta H., Yano H., Young E. D., Zare R. N., Zega T., Ziegler K., Zimmerman L., Zinner E., and Zolensky M. 2006. Comet 81P/Wild 2 under a microscope. *Science* 314:1711–1716.
- Bunch T. E., Becker L., Bada J., Macklin J., Radicatidibrozolo F., Fleming R. H., and Erlichman J. 1993. Hypervelocity impact survivability experiments for carbonaceous impactors, part 2. NASA. Langley Research Center, LDEF: 69 Months in Space. Second Post-Retrieval Symposium. pp. 453–477.
- Bunch T. E., Paque J. M., Becker L., Vedder J. F., and Erlichman J. 1995. Hypervelocity impact survivability experiments for carbonaceous impactors, part 1 NASA. Langley Research Center, LDEF: 69 Months in Space. Third Post-Retrieval Symposium. pp. 385–399.
- Busemann H., Young A. F., Alexander C. M. O. D., Hoppe P., Mukhopadhyay S., and Nittler L. R. 2006. Interstellar chemistry recorded in organic matter from primitive meteorites. *Science* 314:727–730.
- Charnley S. B., Rodgers S. D., Kuan Y., and Huang H. 2002. Biomolecules in the interstellar medium and in comets. *Advances in Space Research* 30:1419–1431.
- Cherchneff I. 1995. Forming dust precursors in the inner envelopes of carbon-rich AGB stars. *Astrophysics and Space Science* 224:379–382.
- Cherchneff I., Barker J. R., and Tielens A. G. G. M. 1992. Polycyclic aromatic hydrocarbon formation in carbon-rich stellar envelopes. *The Astrophysical Journal* 401: 269–287.
- Clairemidi J., Bréchnignac P., Moreels G., and Pautet D. 2004. Tentative identification of pyrene as a polycyclic aromatic molecule in UV spectra of comet P/Halley: An emission from 368 to 384 nm. *Planetary and Space Science* 52:761–772.
- Clemett S. J. 1996. *Complex aromatic molecules in meteorites and interplanetary dust*. Ph.D. thesis, Stanford University, Palo Alto, CA, USA.
- Clemett S. J. and Zare R. N. 1996. Microprobe two-step laser mass spectrometry as an analytical tool for meteoritic samples. In *Molecules in astrophysics: Probes and processes*, IAU Symposium 178, edited by Van Dishoeck E. F. Dordrecht, The Netherlands: Kluwer Academic Publishers. pp. 305–320.
- Clemett S. J., Maechling C. R., Zare R. N., Swan P. D., and Walker R. M. 1993. Identification of complex aromatic molecules in individual interplanetary dust particles. *Science* 262:721–725.

- Clemett S. J., Chillier X. D. F., Gillette S., Zare R. N., Maurette M., Engrand C., and Kurat G. 1998a. Observation of indigenous polycyclic aromatic hydrocarbons in 'giant' carbonaceous antarctic micrometeorites. *Origins of Life and Evolution of the Biosphere* 28:425–448.
- Clemett S. J., Dulay M. T., Gillette J. S., Chillier X. D. F., Mahajan T. B., and Zare R. N. 1998b. Evidence for the extraterrestrial origin of polycyclic aromatic hydrocarbons in the martian meteorite ALH 84001. *Chemistry and Physics of Molecules and Grains in Space: Faraday Discussions* 109:413–436.
- Combi M. R., Harris W. M., and Smyth W. H. 2004. Gas dynamics and kinetics in the cometary coma: theory and observations. In *Comets II*, edited by Festou M. C., Keller H. U., and Weaver H. A. Tucson, AZ: The University of Arizona Press. pp. 523–552.
- Crovisier J. 1994. Photodestruction rates for cometary parent molecules. *Journal of Geophysical Research* 99:3777–3781.
- Davies J. K., Green S. F., and Geballe T. R. 1991. The detection of a strong 3.28-micron emission feature in comet Levy. *Monthly Notices of the Royal Astronomical Society* 251:148–151.
- Duley W. W. and Grishko V. I. 2003. Some 'solid facts' on interstellar dust. *Astrophysics and Space Science* 285:699–708.
- Elsila J. E., De Leon N. P., Buseck P. R., and Zare R. N. 2005. Alkylation of polycyclic aromatic hydrocarbons in carbonaceous chondrites. *Geochimica et Cosmochimica Acta* 69:1349–1357.
- Flynn G. J. and Sutton S. R. 1990. Chemical purity of proposed capture materials: Implications for trace element analyses on captured particles. 21st Lunar and Planetary Science Conference. pp. 371–372.
- Fomenkova M. N. 1999. On the organic refractory component of cometary dust. *Space Science Reviews* 90:109–114.
- Fraya N., Benilan Y., Cottin H., Gazeau M., and Crovisier J. 2005. The origin of the CN radical in comets: A review from observations and models. *Planetary and Space Science* 53:1243–1262.
- Fristrom R. 1995. *Flame structure and processes*. New York: Oxford University Press.
- Gilmour I. 2005. Structural and isotopic analysis of organic matter in carbonaceous chondrites. In *Meteorites, comets and planets*, edited by Davis A. M. Treatise on Geochemistry, vol. 1. Boston: Elsevier. pp. 269–290.
- Hahn J. H., Zenobi R., Bada J. L., and Zare R. N. 1988. Application of two-step laser mass spectrometry to cosmochemistry: Direct analysis of meteorites. *Science* 239:1523–1525.
- Hartmetz C. P., Gibson E. K., and Blanford G. E. 1990a. In situ extraction and analysis of volatiles and simple molecules in interplanetary dust particles, contaminants, and silica aerogel. 21st Lunar and Planetary Science Conference. pp. 343–355.
- Hartmetz C. P., Gibson E. K., Jr., and Lauer H. V. 1990b. A study of aerogel's suitability as an IDP collection substrate: Potential solutions to volatile contamination problems. 21st Lunar and Planetary Science Conference. pp. 463–464.
- Henning T. and Salama F. 1998. Carbon in the universe. *Science* 282:2204–2210.
- Hrubesh L. 1989. Development of low density silica aerogel as a capture medium for hypervelocity particles. Technical Report UCRL-21234. Livermore, CA: Lawrence Livermore National Laboratory.
- Huang H., Gilmour I., Pillinger C. T., and Zolensky M. E. 1993. Removal of carbonaceous contaminants from silica aerogel. 24th Lunar and Planetary Science Conference. pp. 679–680.
- Huang H., Wright I. P., Gilmour I., and Pillinger C. T. 1994. Supercritical fluid extraction as a means of reducing the carbon contamination inherent in samples of silica aerogel destined for the capture of chondritic cosmic dust particles in space. *Planetary and Space Science* 42:947–954.
- Huebner W. F., Boice D. C., and Sharp C. M. 1987. Polyoxymethylene in comet Halley. *The Astrophysical Journal* 320:L149–L152.
- Jenniskens P., Schaller E. L., Laux C. O., Wilson M. A., Schmidt G., and Rairden R. L. 2004. Meteors do not break exogenous organic molecules into high yields of diatomics. *Astrobiology* 4:67–79.
- Joblin C., Boissel P., and De Parseval P. 1997. Polycyclic aromatic hydrocarbon lifetime in cometary environments. *Planetary and Space Science* 45:1539–1542.
- Jones S. M. 2000. Gradient composition sol-gel materials. In *Volume 3943—Sol-gel optics V*, edited by Dunn B. S., Pope E. J., Schmidt H. K., and Yamane M. *Proceedings of SPIE*. pp. 260–269.
- Kearsley A. T., Borg J., Graham G. A., Burchell M. J., Cole M. J., Leroux H., Bridges J. C., Hörz F., Wozniakiewicz P. J., Bland P. A., Bradley J. P., Dai Z. R., Teslich N., See T., Hoppe P., Heck P. R., Huth J., Stadermann F. J., Floss C., Marhas K., Stephan T., and Leitner J. 2008. Dust from comet Wild 2: Interpreting particle size, shape, structure, and composition from impact features on the Stardust aluminum foils. *Meteoritics & Planetary Science* 43:41–73.
- Keller L. P., Messenger S., Miller M., and Thomas K. L. 1997. Nitrogen speciation in a <sup>15</sup>N-enriched interplanetary dust particle. 28th Lunar and Planetary Science Conference. pp. 707–708.
- Kissel J. and Krueger F. R. 1987. The organic component in dust from comet Halley as measured by the PUMA mass spectrometer on board VEGA 1. *Nature* 326:755–760.
- Kissel J., Krueger F. R., Silen J., and Clark B. C. 2004. The cometary and interstellar dust analyzer at comet 81P/Wild 2. *Science* 304:1774–1776.
- Kissel J., Krueger F. R., and Silen J. 2005. Analysis of Cosmic Dust by the 'Cometary and Interstellar Dust Analyser' (CIDA) Onboard the Stardust Spacecraft. In *Dust in Planetary Systems, Conference Proceedings, Kauai, Hawaii, LPI Contribution No. 1280*, p. 95.
- Koidl P., Wild C., Dischler B., Wagner J., and Ramsteiner M. 1989. Plasma deposition, properties and structures of amorphous hydrogenated carbon films. *Materials Science Forum* 52-53:41–70.
- Korth A., Marconi M. L., Mendis D. A., Krueger F. R., Richter A. K., Lin R. P., Mitchell D. L., Anderson K. A., Carlson C. W., Reme H., Sauvaud J. A., and D'Uston C. 1989. Probable detection of organic-dust-borne aromatic C<sub>3</sub>H<sub>3</sub><sup>+</sup> ions in the coma of comet Halley. *Nature* 337: 53–55.
- Korth A., Krueger F. R., Mendis D. A., and Mitchell D. L. 1990. Organic ions in the coma of comet Halley. In *Asteroids, comets, meteors III*, edited by Lagerkvist C. I.,

- Rickman H., and Lindblad B. A. Uppsala: Universitet. 373 p.
- Kovalenko K. L., Maechling C. R., Clemett S. J., Phillopoz J., Zare R. N., and Alexander C. 1992. Microscopic organic analysis using two-step laser mass spectrometry: Application to meteoritic acid residues. *Analytical Chemistry* 64:682–690.
- Krueger F. R. and Kissel J. 2006. Interstellar and cometary dust in relation to the origin of life. In *Comets and the origin and evolution of life, advances in astrobiology and biogeophysics*, edited by Thomas P. J., Hicks R. D., Chyba C. F., and McKay C. P. Berlin/Heidelberg: Springer. pp. 325–339.
- Leger A. and Puget J. L. 1984. Identification of the 'unidentified' IR emission features of interstellar dust? *Astronomy and Astrophysics* 137:L5–L8.
- Lerner E. J. 2004. Less is more with aerogels. *The Industrial Physicist* October/November:28–32.
- Levasseur-Regourd A. C. and Desvoivres E. 2004. Comets and the origin of life: Structure of comets, nuclei and dust. In *Bioastronomy 2002: Life among the stars: Proceedings of the 213th Symposium of the IAU*, edited by Norris R. P. and Stootman F. H. San Francisco: Astronomy Society of the Pacific. pp. 213–271.
- Lodders K. and Osborne R. 1999. Perspectives on the comet-asteroid-meteorite link. *Space Science Reviews* 90: 289–297.
- McKay D. S., Gibson E. K., Thomas-Keptra K. L., Vali H., Romanek C. S., Clemett S. J., Chiller X. D. F., Maechling C. R., and Zare R. N. 1996. Search for past life on Mars: Possible relic biogenic activity in martian meteorite ALH 84001. *Science* 273:924–930.
- McKeegan K. D., Aléon J., Bradley J., Brownlee D., Busemann H., Butterworth A., Chaussidon M., Fallon S., Floss C., Gilmour J., Gounelle M., Graham G., Guan Y., Heck P. R., Hoppe P., Hutcheon I. D., Huth J., Ishii H., Ito M., Jacobsen S. B., Kearsley A., Leshin L. A., Liu M.-C., Lyon I., Marhas K., Marty B., Matrajt G., Meibom A., Messenger S., Mostefaoui S., Mukhopadhyay S., Nakamura-Messenger K., Nittler L., Palma R., Pepin R. O., Papanastassiou D. A., Robert F., Schlutter D., Snead C. J., Stadermann F. J., Stroud R., Tsou P., Westphal A., Young E. D., Ziegler K., Zimmermann L., and Zinner E. 2006. Isotopic compositions of cometary matter returned by Stardust. *Science* 314:1724–1728.
- Meech K. J. and Bauer J. M. 2004. Comets and the connection to life. In *Bioastronomy 2002: Life among the stars: Proceedings of the 213th Symposium of the IAU*, edited by Norris R. P. and Stootman F. H. San Francisco: Astronomical Society of the Pacific. pp. 263.
- Mekenyan O. G., Ankley G. T., Veith G. D., and Call D. J. 1994. QSARs for photoinduced toxicity: I. Acute lethality of polycyclic aromatic hydrocarbons to *Daphnia magna*. *Chemosphere* 28:567–582.
- Messenger S., Amari S., Gao X., Walker R. M., Clemett S. J., Chiller X. D. F., Zare R. N., and Lewis R. S. 1998. Indigenous polycyclic aromatic hydrocarbons in circumstellar graphite grains from primitive meteorites. *The Astrophysical Journal* 502:284–295.
- Mimura K., Okamoto M., Sugitani K., and Hashimoto S. 2007. Selective release of D and <sup>13</sup>C from insoluble organic matter of the Murchison meteorite by impact shock. *Meteoritics & Planetary Science* 42:307–474.
- Moreels G., Clairemidi J., Hermine P., Brechignac P., and Rousselot P. 1994. Detection of a polycyclic aromatic molecule in comet P/Halley. *Astronomy and Astrophysics* 282:643–656.
- Mumma M. J., Weissman P. R., and Stern S. A. 1993. Comets and the origin of the solar system—Reading the Rosetta stone. In *Protostars and planets III*, edited by Levy E., Lunine J. I., Matthews M. S., and Guerrieri M. L. Tucson, AZ: The University of Arizona Press. pp. 1177–1252.
- Nakamura-Messenger K., Messenger S., Keller L. P., Clemett S. J., and Zolensky M. E. 2006. Organic globules in the Tagish Lake meteorite: Remnants of the protosolar disk. *Science* 314:1439–1442.
- Pearson V. K., Sephton M. A., and Gilmour I. 2006. Molecular and isotopic indicators of alteration in CR chondrites. *Meteoritics & Planetary Science* 41:1291–1303.
- Pizzarello S., Cooper G. W., and Flynn G. J. 2006. The Nature and distribution of the organic material in carbonaceous chondrites and interplanetary dust particles. In *Meteorites and the early solar system II*, edited by Lauretta D. S. and McSween H. Y., Jr. Tucson, AZ: The University of Arizona Press. pp. 625–651.
- Rairden R. L., Jenniskens P., and Laux C. O. 2000. Search for organic matter in Leonid meteoroids. *Earth, Moon, and Planets* 82–83:71–80.
- Rettig T. W., Tegler S. C., Pasto D. J., and Mumma M. J. 1992. Comet outbursts and polymers of HCN. *The Astrophysical Journal* 398:293–298.
- Sago K. and Hattori T. 1996. Identification and removal of trace organic contamination on silicon wafers stored in plastic boxes. *Journal of the Electrochemical Society* 143:3279–3284.
- Salama F., Galazutdinov G. A., Krelowski J., Allamandola L. J., and Musaev F. A. 1999. Polycyclic aromatic hydrocarbons and the diffuse interstellar bands: A survey. *The Astrophysical Journal* 526:265–273.
- Sandford S. A., Allamandola L. J., Tielens A. G. G. M., Sellgren K., Tapia M., and Pendleton Y. 1992. The interstellar C–H stretching band near 3.4 microns: Constraints on the composition of organic material in the diffuse interstellar medium. *The Astrophysical Journal* 371:607–620.
- Sandford S. A., Aléon J., Alexander C. M. O' D., Araki T., Bajt S., Baratta G. A., Borg J., Bradley J. P., Brownlee D. E., Brucato J. R., Burchell M. J., Busemann H., Butterworth A., Clemett S. J., Cody G., Colangeli L., Cooper G., D'Hendecourt L., Djouadi Z., Dworkin J. P., Ferrini G., Fleckenstein H., Flynn G. J., Franchi I. A., Fries M., Gilles M. K., Glavin D. P., Gounelle M., Grossemy F., Jacobsen C., Keller L. P., Kilcoyne A. L. D., Leitner J., Matrajt G., Meibom A., Mennella V., Mostefaoui S., Nittler L. R., Palumbo M. E., Papanastassiou D. A., Robert F., Rotundi A., Snead C. J., Spencer M. K., Stadermann F. J., Steele A., Stephan T., Tsou P., Tylliszczak T., Westphal A. J., Wirick S., Wopenka B., Yabuta H., Zare R. N., and Zolensky M. E. 2006. Organics captured from comet 81P/Wild 2 by the Stardust spacecraft. *Science* 314:1720–1724.
- Scholl H. and Froeschle C. 1977. The Kirkwood gaps as an asteroidal source of meteorites. In *IAUC 39: Comets, asteroids, meteorites: Interrelations, evolution and origins*,

- edited by Delsemme A. H. Toledo: University of Toledo. pp. 293–295.
- Sephton M. A. 2005. Organic matter in carbonaceous meteorites: Past, present and future research. *Royal Society of London Transactions Series A* 363:2729–2742.
- Sephton M. A. and Gilmour I. 2000. Aromatic moieties in meteorites: Relics of interstellar grain processes? *The Astrophysical Journal* 540:588–591.
- Sephton M. A., Verchovsky A. B., and Wright I. P. 2004. Carbon and nitrogen isotope ratios in meteoritic organic matter: Indicators of alteration processes on the parent asteroid. *International Journal of Astrobiology* 3:221–227.
- Spencer M. K. and Zare R. N. 2007. Comment on ‘organics captured from comet 81P/Wild 2 by the Stardust spacecraft. *Science* 317:1680c.
- Strazzulla G. 1999. Ion irradiation and the origin of cometary materials. *Space Science Reviews* 90:269–274.
- Thomas P. J., Chyba C. F., McKay C. P., and Hicks R. D. 2006. Comets and the origin and evolution of life. In *Comets and the origin and evolution of life*, edited by Thomas P. J., Chyba C. F., McKay C. P., and Hicks R. D. Berlin: Springer. pp. 169–206.
- Tobiska W. K. 2004. Solar2000 irradiances for climate change research, aeronomy and space system engineering. *Advances in Space Research* 34:1736–1746.
- Tsou P., Brownlee D. E., Sandford S. A., Hörz F., and Zolensky M. E. 2003. Wild 2 and interstellar sample collection and Earth return. *Journal of Geophysical Research (Planets)* 108:8113–8123.
- Woods P. M. and Willacy K. 2007. Benzene formation in the inner regions of protostellar disks. *The Astrophysical Journal* 655:L49–L52.
- Zenobi R., Philippoz J., Zare R. N., and Buseck P. R. 1989. Spatially resolved organic analysis of the Allende meteorite. *Science* 246:1026–1029.
- Zenobi R., Philippoz J., Zare R. N., Wing M. R., Bada J. L., and Marti K. 1992. Organic compounds in the Forest Vale, H4 ordinary chondrite. *Geochimica et Cosmochimica Acta* 56:2899–2905.
-